UNIVERSITÀ
DEGLI STUDI
DI PADOVA

DIPARTIMENTO
DI INGEGNERIA
DELL'INFORMAZIONE

DIPARTIMENTO DI INGEGNERIA DELL'INFORMAZIONE

CORSO DI LAUREA MAGISTRALE IN

BIOINGEGNERIA

"MODELING AND CONTROL OF LOOP DIURETIC THERAPY IN CONGESTIVE HEART FAILURE: A FEASIBILITY STUDY"

Relatore: Prof. Simone Del Favero

Laureanda: Corinna Semenzato

Correlatore: Dott. Giacomo Rossitto

ANNO ACCADEMICO 2022 – 2023

Data di laurea 21 Aprile 2023

Abstract

Congestive heart failure (CHF) is a condition caused by the heart's inability to correctly circulate blood to peripheral tissues, which results in a persistent state of increased plasma volume, due to the overactivation of neurohumoral complexes that induce the body to retain renal sodium and water.

The most common therapy for decongestion is the administration of diuretics, in particular loop diuretics such as furosemide. Since the effects of diuretic drugs in case of CHF can largely vary between patients, the actual course of the treatment is not standardised, and its efficacy relies on the physician's expertise.

This work aimed to implement a control system, using a model predictive control (MPC) strategy, that could automatically and dynamically adapt the administration of furosemide by predicting the patient's response to the treatment based on the patient's characteristics, in order to achieve decongestion more efficiently than with standard therapy.

As part of the simulation set up, literature was extensively consulted in the search for a pharmacokinetic and pharmacodynamic (PKPD) model of furosemide, finally settling on a three-compartment representation of the pharmacokinetics and a four-parameters sigmoidal pharmacodynamic response that describes the urine production in response to the drug.
In addition to that, a mathematical model of renal activity was needed. Two models were shortlisted. One, more articulated and capable of describing several physiological events, was discarded because it was too complex to integrate with the PKPD model. The second model was simpler and described a first-order, negative-feedback response of the kidneys to changes in plasma volume from its normal physiological level, which could be easily integrated with the furosemide PKPD model.

Once the control simulation was set up, results showed that an automated MPC-controlled diuretic administration can outperform standard diuretic treatment in case of congestive heart failure by achieving comparatively higher level of decongestion in less time.

Contents

Chapter 1

Introduction

Heart failure (HF) is one of the most common causes for hospitalisation, especially in elder population. In the United Kingdom alone, in 2019 more than 100,000 hospital admissions were associated with heart failure, in a growing trend that was only stopped by the dramatic emergence of the Covid-19 pandemic[1].

A common by-product of HF is fluid overload, in which case the condition is known as congestive heart failure (CHF)[2]. Fluid retention can cause the activation of neurohumoral complexes that induces a state of increased renal sodium and water avidity that results in an increased plasma volume, which then induces the further activation of the same neurohumoral complexes, causing the further worsening of the patient's prognosis[3] (see Figure 1.1).

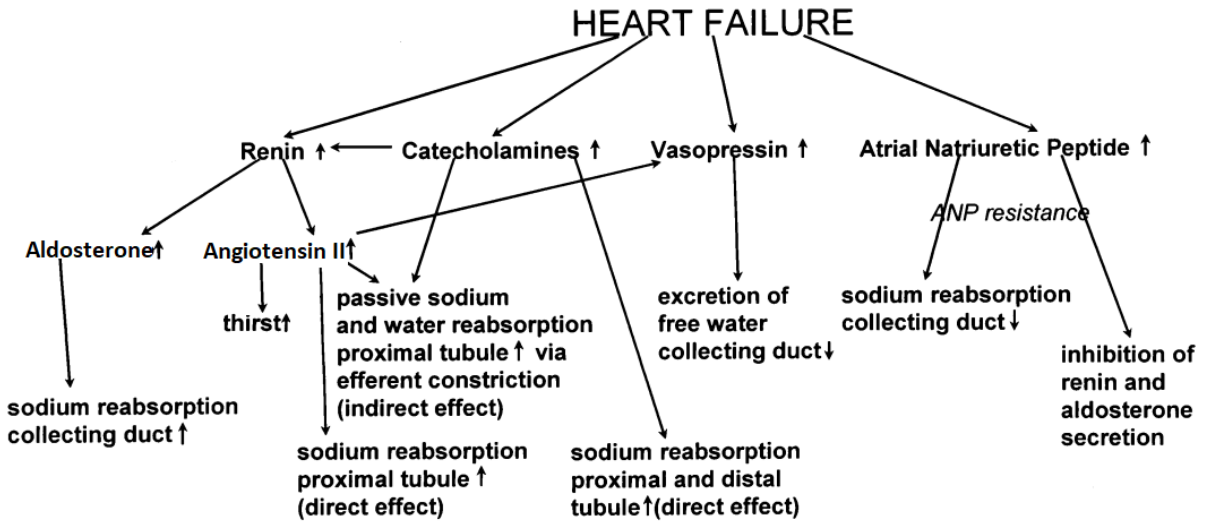

Figure 1.1: *Mechanisms of sodium and water retention in patients with heart failure, adapted from[4].*

The most common approach for decongestion therapy in CHF patients is the adminis-

tration of diuretic drugs. In particular, the first and most common approach requires the use of a specific class of diuretics, the so-called loop diuretics, whose site of action is the loop of Henle (Fig. 2.2). This approach, however, is undermined by the varied efficacy of diuretics on CHF patients, deriving from their own decompensated renal function. This results in the treatment plan being mostly dependent on the physician's expertise[3, 4].

Our aim with this work is to devise, tune, and test an automated control system capable of adapting a CHF patient's diuretic treatment based on the patient's own physiology in order to achieve a more efficient decongestion than what the standard clinical therapy can offer. Particularly, we have elected to use a model predictive control (MPC) strategy, which has already proven effective for automated insulin delivery in type-1 diabetic patients[5, 6].

The most common loop diuretics are furosemide, torsemide, and bumetanide. We will focus on the therapeutic effects of furosemide, since it is the chosen loop diuretic at the Padua Univesity Hospital.

Chapter 2

Introduction to Renal Physiology

In order to understand the quantities and phenomenons involved in controlling the decongestion process, we need to establish some ground knowledge about renal physiology, since the kidneys are the prime actors in the control of the balance of most body fluids.

2.1 Osmoregulation

Kidneys are the principal players in osmoregulation, which is the maintenance and regulation of the organism's internal balance, known as homeostasis, by the organism itself in regards to the dynamic equilibrium between fluids and dissolved materials such as electrolytes[7].

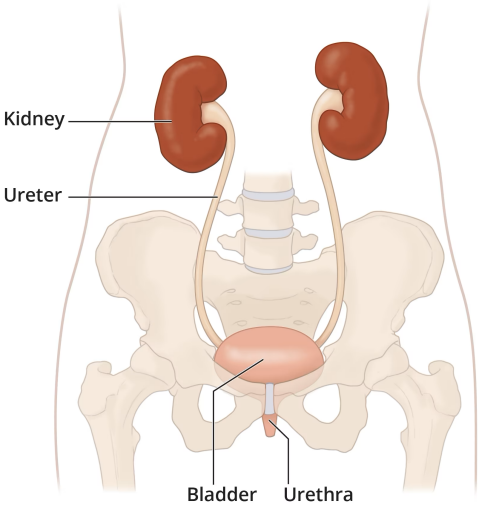

Figure 2.1: *Components of the urinary tract[8].*

Kidneys manage that balance through the control of body fluid volume, electrolyte concentration, acid-base balance, and fluid osmolarity, by filtrating waste material out of blood. The product of renal filtration is urine, which flows into two muscular tubes, the ureteres, to be accumulated in the bladder. Kidneys, ureters, and the bladder are part of the urinary tract.
Healthy kidneys can filter about 150ml of blood every minute[8, 9].

2.1.1 Renal filtration

The functional unit of the kidney is the nephron, depicted in Figure 2.2. Each kidney has over a million nephrons working simultaneously.
Each nephron can be functionally divided into two main components: Bowman's capsule

and the tubule.

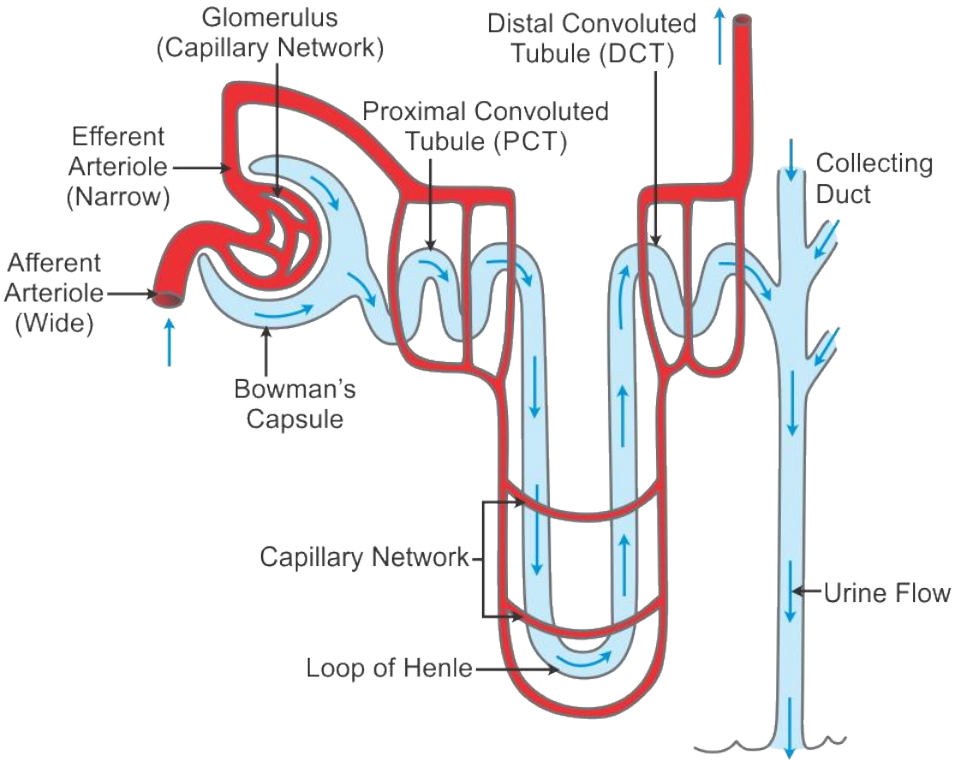

Figure 2.2: *Model representation of a nephron[10].*

Bowman's capsule is the blind end of the tubule that wraps around a cluster of blood capillaries, called the glomerulus. The blood in the glomerulus is grossly filtered by passing through the layers that make up the wall structure of Bowman's capsule. The product of this first filtration is called ultrafiltrate. It is mostly a by-product of plasma and is low in protein.

The ultrafiltrate collected in Bowman's capsule passes then through the three sections of the tubule: the proximal tubule, the loop of Henle, and the distal tubule. In the tubules the composition of the ultrafiltrate is further modified through the reabsorption and secretion of those substances, such as electrolytes and proteins, that the body needs to either preserve or excrete. The different sections of the tubules have different mechanisms of reabsorption and secretion, as well as preferred target molecules, but for the purposes of this thesis, we will not need to explore in depth these differences.

Once the ultrafiltrate has passed through the tubule, it arrives to the collecting duct, which collects the product out of several nephrons and leads the newly-made urine to the ureters which take it out of the kidneys and onto the bladder, waiting for excretion through urination[9].

2.1.2 Hormonal regulation

The reabsorption of fluid and electrolytes is modulated by hormones, such as angiotensin II, aldosterone, and the antidiuretic hormone (ADH).

The main role of ADH, also known as vasopressin, is the maintenance of blood pressure and the conservation of fluid volume in order to keep a stable osmolarity by promoting water reabsorption and reducing urine output by the kidneys. The release of ADH is extremely easy to trigger, because it is stored inside neurons within the hypothalamus which possess extremely responsive osmoreceptors that promote the secretion of ADH in response even to slight elevations in osmolarity[11, 12].

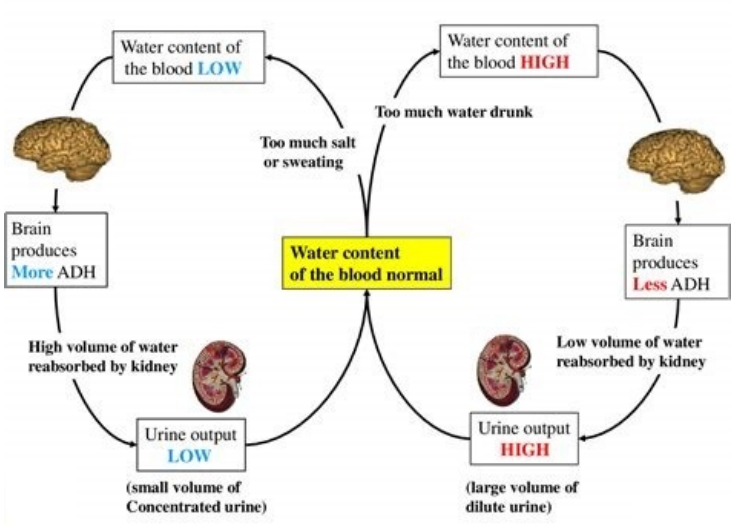

Figure 2.3: *ADH schematic[13].*

The renin-angiotensin-aldosterone system (RAAS) consists in a hormonal interplay that mainly aims to regulate sodium and potassium balance, fluid volume, and blood pressure. Its activity affects not only renal activity, but also the brain and the circulatory system. Among other things, excessive activation of RAAS increases the risk of cardiovascular diseases.

Renin is an enzyme produced by the kindey. Its main purpose is the conversion in the liver of a protein, angiotensinogen, that activates the angiotensin I hormone which starts a catalytic reaction that ends in the production of the angiotensin II hormone.

Angiotensin II has several effects on the organisms, such as inducing vase constriction, therefore increasing blood pressure, and promoting the release of ADH and aldosterone[14].

The main biological action of aldosterone is the promotion of sodium retention by stimulating the opening of ion channels along the renal tubules that allow for the reabsorption of sodium into the blood stream in exchange for potassium, which in turn gets expelled into the urine[15, 16, 17].

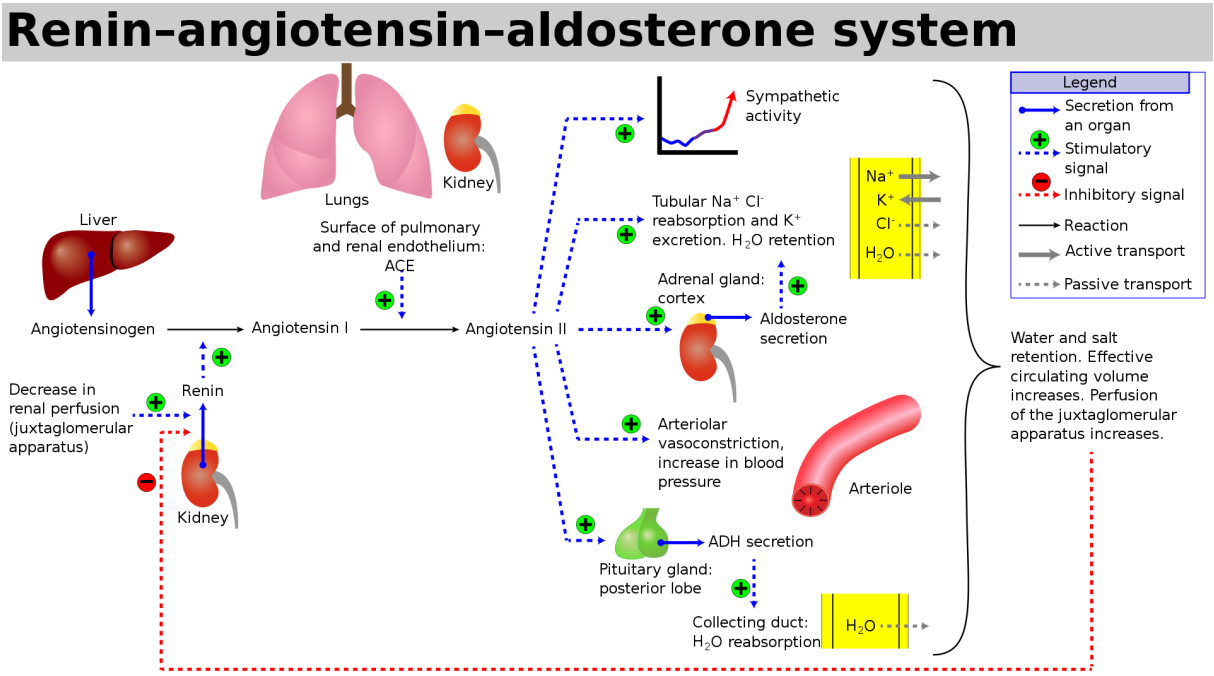

Figure 2.4: *RAAS schematic[18].*

2.2 Mechanisms of action of furosemide

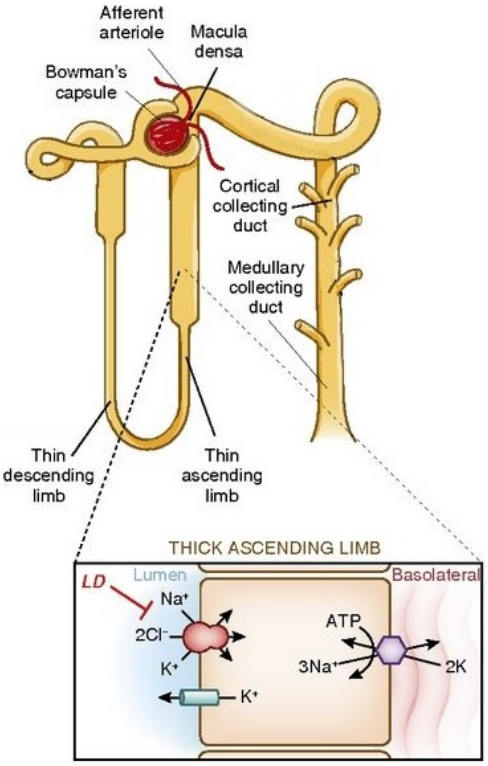

Figure 2.5: *Furosemide site of action in the nephron, adapted from [19].*

The site of action of furosemide, as is the case for all loop diuretics, is the ascending loop of Henle.

The molecule of furosemide is capable of binding to the active site of the Na-K-2Cl (NKCC2) cotransporter, thus inhibiting its ability to transport sodium and chloride ions from the luminal side of the renal tubule back into the blood stream. The blockade leads to a imbalance in osmotic pressure that induces increased water excretion through a higher urine production[15, 19, 20].

The self-regulatory mechanisms of the kidney allow our bodies to recoup most of the Na^+ that is blocked in the loop of Henle, through reabsorption in the distal tubule, while most of the water content in the filtrate is trapped in the tubule and is channelled into the collecting duct, increasing urine volume[21].

Once challenge that is tied to the use of furosemide, is that the kidney can adapt to its presence, as well as to that of other diuretic drugs, countering its effect even after one administration[19, 21], thanks to a physiological phenomenon called diuretic braking. Figure 2.6 gives for a visual representation of how the effectiveness of loop diuretics is affected by repeated consecutive doses.

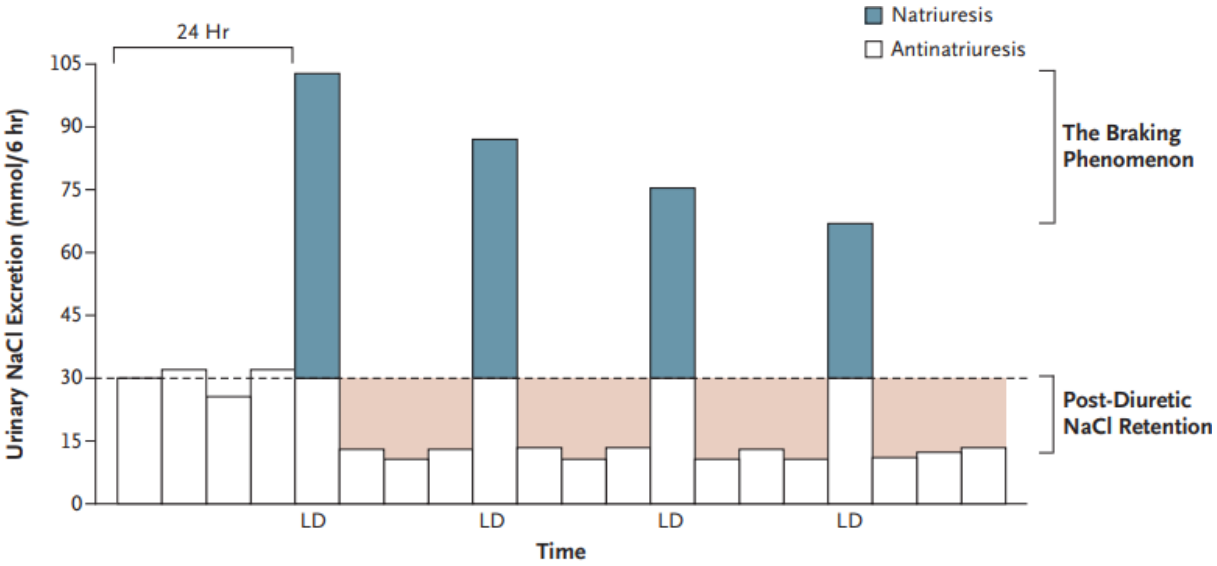

Figure 2.6: *From[19]: Effects of repeated daily doses of a loop diuretic (LD) on NaCl excretion, viewed in 6-hour blocks. Post-diuretic NaCl retention and the braking phenomenon are shown. Natriuresis must exceed antinatriuresis to be of any effect.*

Chapter 3

Furosemide PKPD Modeling

3.1 Pharmacokinetics

In order to apply a model-based control strategy such as model predictive control, we need a model that describes the patient, the drugs injected, and their interactions. This is commonly achieved through the use of pharmacokinetic-pharmacodynamic (PKPD) modelling.

The pharmacokinetic (PK) model of a drug quantitatively describes how body interacts with administered substances for the entire duration of exposure, which is to say "what the body does to the drug". In particular, it examines the process of absorption, distribution, and elimination of the drug in the body[22].

The pharmacokinetics of furosemide administered intravenously are effectively described by a three-compartment model with zero-order input and first order elimination[23]. As shown in Figure 3.1, the three-compartment model includes a central compartment, which describes the plasma concentration of the drug, and two peripheral compartments that represent respectively highly and scarcely perfused tissues. The fourth compartment represents the quantity of furosemide collected in urine. The output of interest of our PK model is the urinary excretion rate of the drug.

The differential equations derived from the compartmental model are

$$\begin{cases} \dot{Q}_c(t) = k_{21}Q_{p1}(t) + k_{31}Q_{p2}(t) - (k_{14} + k_{NR} + k_{12} + k_{13})Q_c(t) + k_0 D_{i.v.} \\ \dot{Q}_{p1}(t) = k_{12}Q_c(t) - k_{21}Q_{p1}(t) \\ \dot{Q}_{p2}(t) = k_{13}Q_c(t) - k_{31}Q_{p2}(t) \\ \dot{Q}_u(t) = k_R Q_c(t) \end{cases} \tag{3.1}$$

where the distribution rates are

$$k_{12} = \frac{CL_{p1}}{V_c} \quad k_{21} = \frac{CL_{p1}}{V_{p1}} \quad k_{13} = \frac{CL_{p2}}{V_c} \quad k_{31} = \frac{CL_{p2}}{V_{p2}} \quad k_R = \frac{CL_R}{V_c} \quad k_{NR} = \frac{CL_{NR}}{V_c}$$

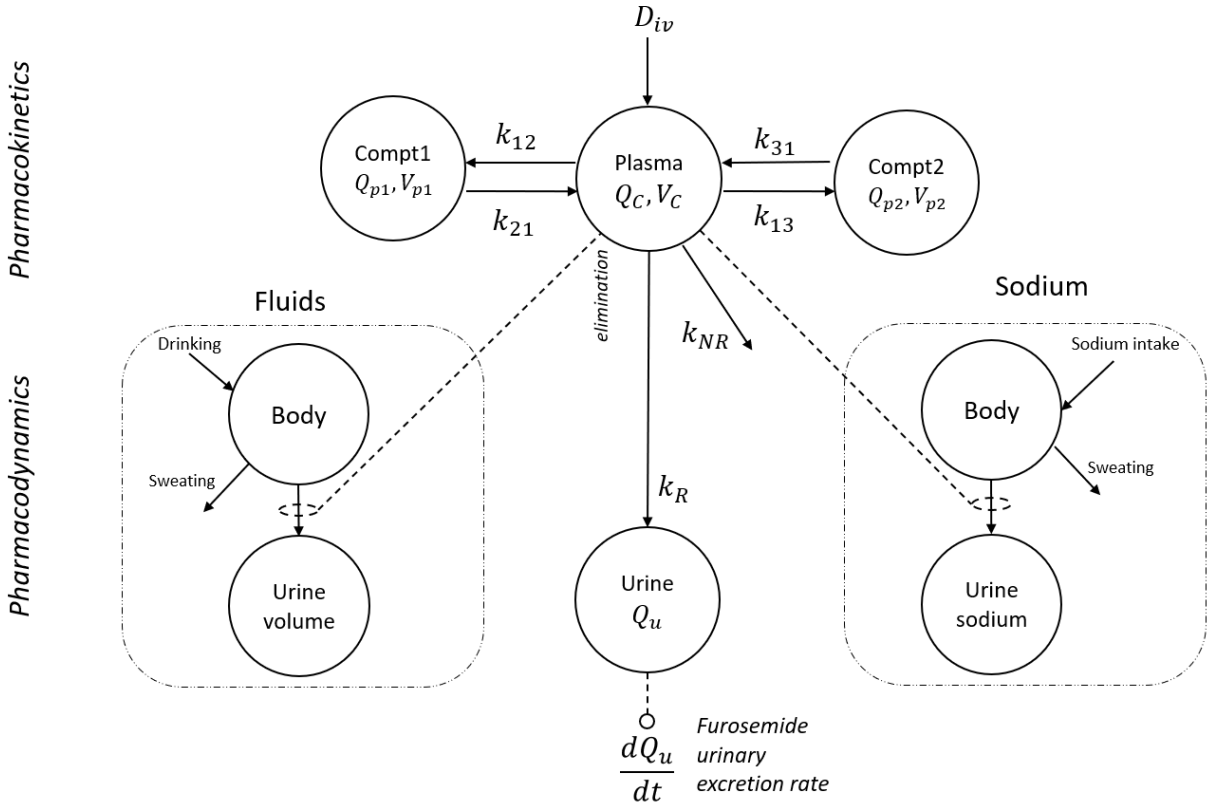

Figure 3.1: *Furosemide PKPD compartmental model*

$D_{i.v.}$ is the dose in milligrams of furosemide injected intravenously as a bolus; Q_c, Q_u, Q_{p1}, and Q_{p2} describe the amount in milligrams of furosemide stored respectively in plasma, urine, and the two peripheral compartments; V_c [L] is the central volume of distribution of the drug; CL_R and CL_{NR} [L/h] are the renal and non-renal clearances, respectively; V_{p1}, V_{p2}, CL_{p1}, and CL_{p2} represent the volume of distribution [L] and the distribution clearance [L/h] of each peripheral compartment.

The PK parameters estimated in [23] are reported in Table 3.1. Variability (mean ± std) has been taken from the same work, where it was derived using a bootstrapping approach.

Table 3.1: *PK parameters*

CL_R	3.97 ± 0.21	L/h	V_c	5.97 ± 0.84	L
CL_{p1}	1.10 ± 0.23	L/h	V_{p1}	18.1 ± 5.85	L
CL_{p2}	2.55 ± 0.69	L/h	V_{p2}	3.01 ±0.43	L
CL_{NR}	2.02 ± 0.32	L/h			

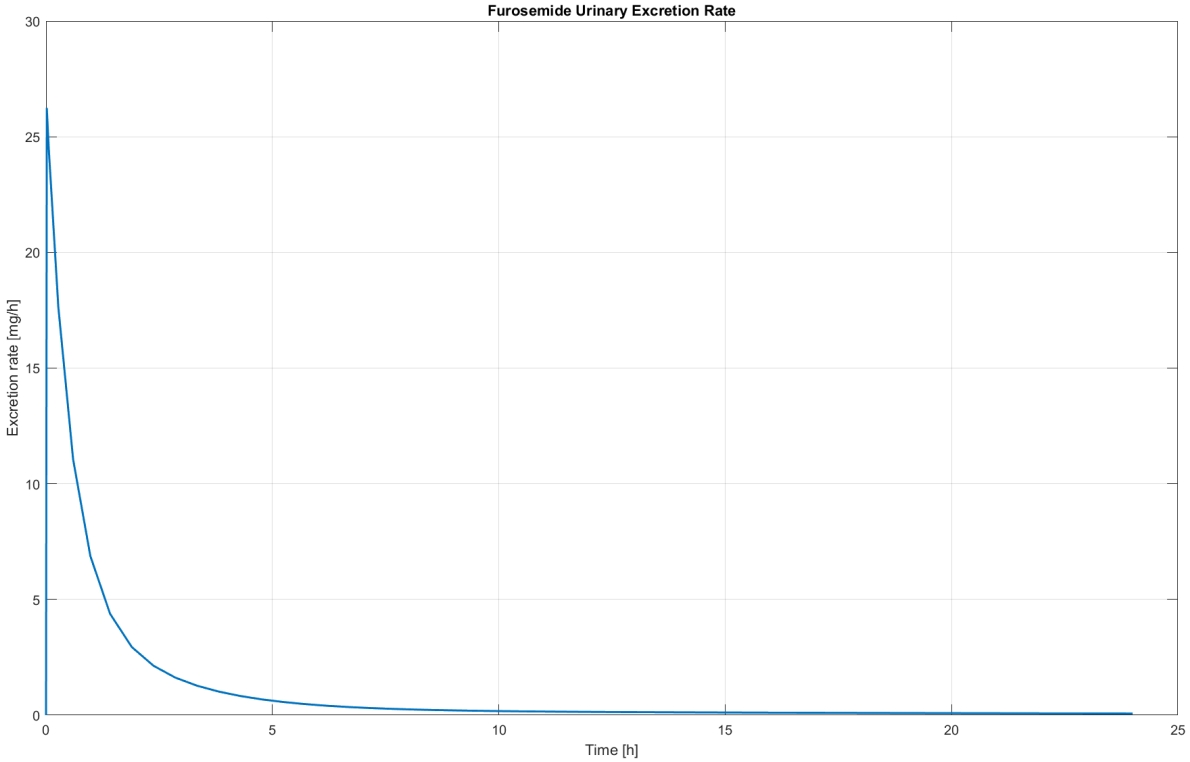

Figure 3.2: *Furosemide pharmacokinetics: urinary excretion rate after one dose of 40mg of furosemide.*

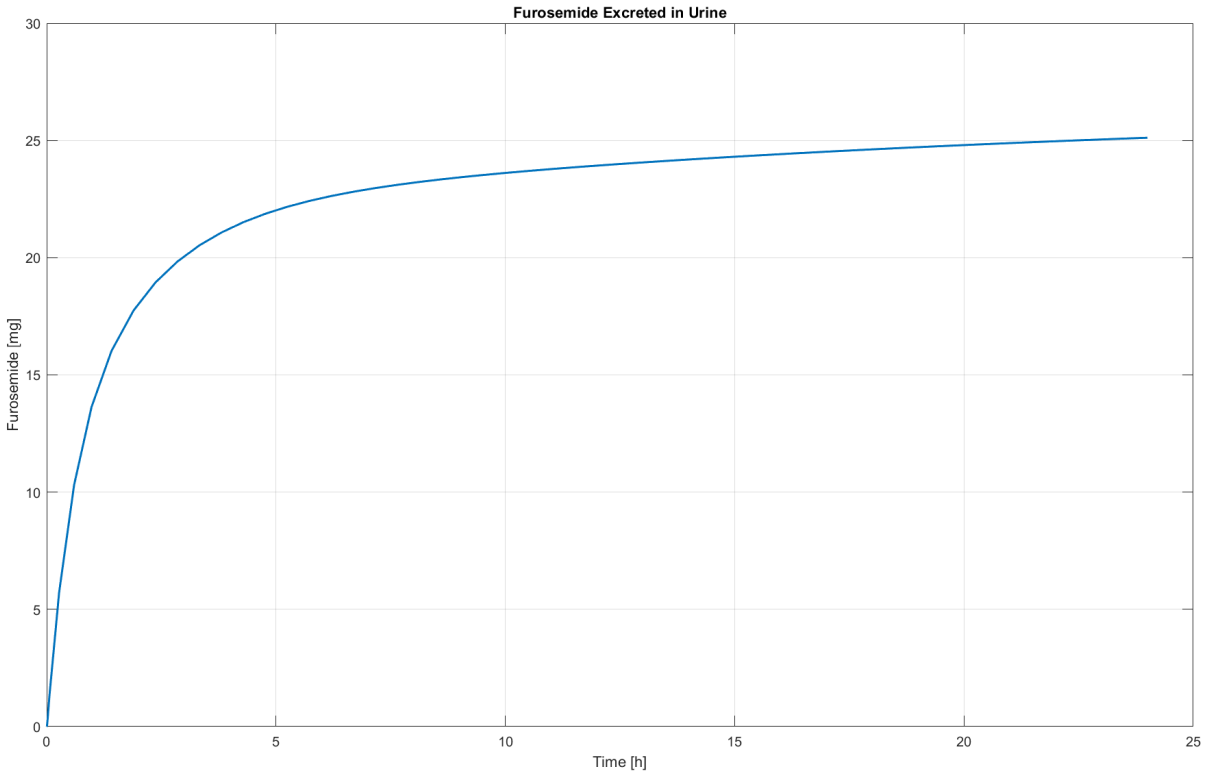

Figure 3.3: *Furosemide pharmacokinetics: cumulative amount of furosemide excreted in urine after one dose of 40mg of furosemide.*

3.2 Pharmacodynamics

Pharmacodynamics (PD) describes the biochemical, physiologic, and molecular effects effects that the drug has on the tissue of action and, more generally, the whole body. Where pharmacokinetics deals with "what the body does to the drug", pharmacodynamics explores "what the drug does to the body".[24]

In our case, we know that, when active, furosemide binds to the Na-K-2Cl (NKCC2) symporter from the luminal side, inhibiting its ability to reabsorb sodium at the loop of Henle. This causes an increase in both water and sodium excretion.

The observed pharmacodynamics can be characterised by a 4-parameter sigmoidal function[25]:

$$Y = \frac{a - d}{1 + (\frac{X}{c})^b} + d \tag{3.2}$$

Where Y is the measure of interest, either sodium or urine excretion rate; X is the furosemide urinary excretion rate, which is derived from the PK model; a is the baseline excretion rate of the response measure at zero furosemide excretion; b is the slope factor; c is the furosemide excretion rate resulting from ED_{50}; and d is the excretion rate of the response measure at an infinite furosemide excretion rate.

Given the appropriate sets of parameters, Equation 3.2 can describe either the sodium or the urine excretion response, because both follow the same behaviour in response to furosemide.

The review done by Ponto and Schenwald[25] reports values from different studies that examined the PD response in normal subjects, CHF patients, and patients with chronic renal insufficiency. The average values of the parameters for subjects with CHF are reported in Table 3.2.

Table 3.2: *PD parameters for average CHF patient*

Response	a	b	c	d
Urine volume	[L/h]		[mg/h]	[L/h]
	$(4.47 \pm 0.78) \cdot 10^{-2}$	1.63 ± 0.05	4.46 ± 1.43	0.54 ± 0.07
Sodium response	[mmol/h]		[mg/h]	[mmol/h]
	$(3.06 \pm 4.40) \cdot 10^{-4}$	1.80 ± 0.31	5.55 ± 1.83	$(1.66 \pm 0.74) \cdot 10^{-2}$

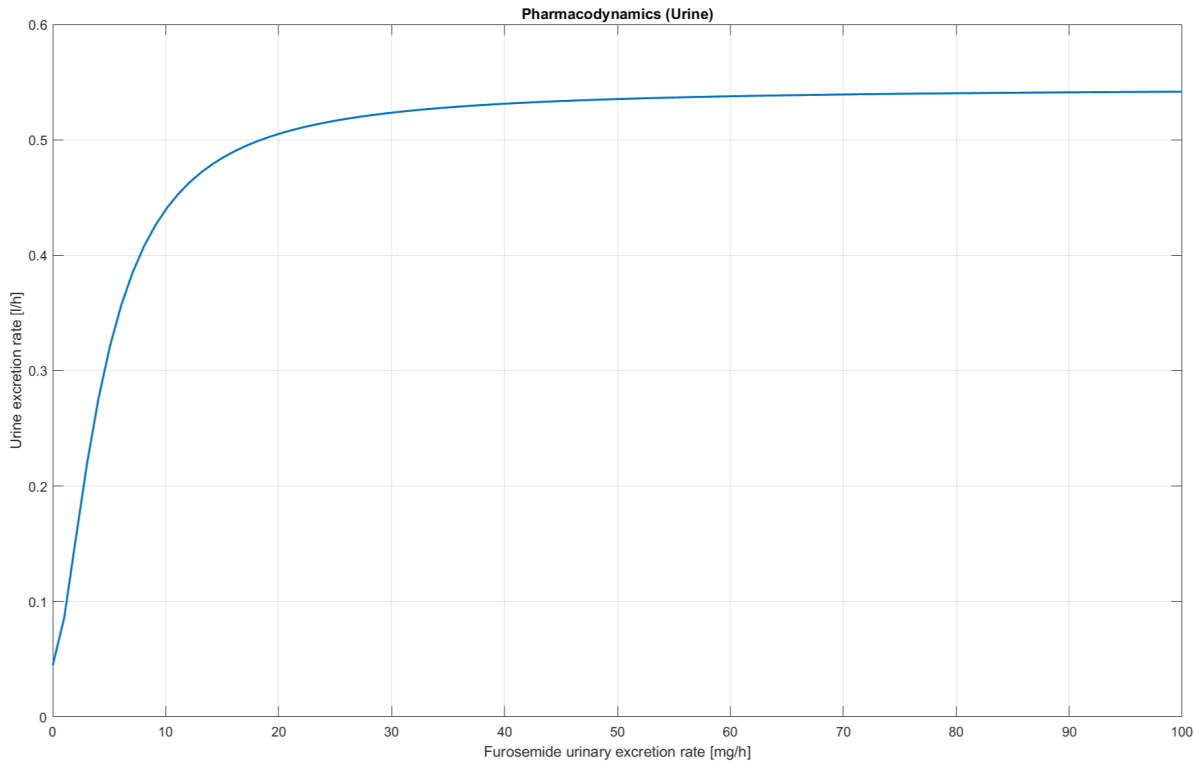

Figure 3.4: *Sweep response of Equation 3.2 for the average patient*

3.3 Simulated population

The population analysis performed by Van Wart et al.[23] identified that the most statistically significant covariate to individualise this model is the subject's level of renal functionality, which can be modelled through creatinine clearance CL_{Cr} [mL/min], a quantity that can be estimated using the Cockcroft-Gault formula (Equation 3.3, which requires standard anthropometric data and a measurement of serum creatinine S_{Cr} [mg/dL]:

$$CL_{Cr} = \frac{(140 – age) \cdot weight}{72 \cdot S_{Cr}} (\cdot 0.85 \text{ if female}) \tag{3.3}$$

It stands to reason that renal functionality has a direct impact on CL_R, and therefore on the behaviour of furosemide, since its site of action is the kidney. The relationship between CL_R and CL_{Cr} can be approximated with a linear function:

$$CL_R \approx 0.039 \cdot CL_{Cr} \tag{3.4}$$

Although compromised kidney function is often a by-product of heart failure, for this work, we elected to consider patients with normal renal function, also considering that a sever impairment of the renal system would have required extensive adjustments to the kidney model discussed in Chapters 4 and 5.

The pharmacodynamics of furosemide are much more variable than the pharmacokinetics, and at the moment, a complete population analysis for the PD model in literature doesn't exist. For what concerns the creation of a simulated population dataset, we have assumed that all parameters follow a Gaussian distribution.
We also decided to not consider the sodium excretion, because of the impossibility to find a model of renal function that could describe both the overall urine excretion as well as the electrolyte content in urine.

The parameters for the simulated population are reported in Tables 3.3 and 3.4.

Table 3.3: *PK Population parameters*

Subject	Cl_R [L/h]	Cl_{NR} [L/h]	V_C [L]	Cl_{d1} [L/h]	V_{d1} [L]	Cl_{d2} [L/h]	V_{d2} [L]
0	3.97	2.02	5.97	1.10	18.10	2.55	3.01
1	3.87	1.97	5.82	1.07	7.91	0.89	2.93
2	3.93	2.00	5.91	1.09	17.92	2.94	2.98
3	4.04	2.05	6.07	1.12	20.00	4.20	3.06
4	5.02	2.55	7.55	1.39	12.74	2.62	3.81
5	3.37	1.71	5.07	0.93	17.89	2.95	2.56
6	5.37	2.73	8.08	1.49	30.76	3.37	4.07
7	4.14	2.10	6.22	1.15	24.03	2.76	3.14
8	2.74	1.39	4.12	0.76	15.57	3.29	2.08
9	4.72	2.40	7.10	1.31	13.87	3.49	3.58
10	5.15	2.62	7.74	1.43	16.47	1.78	3.90
11	2.69	1.37	4.05	0.75	12.50	2.94	2.04
12	3.79	1.93	5.70	1.05	21.07	3.34	2.87
13	5.04	2.57	7.58	1.40	16.00	2.59	3.82
14	3.26	1.66	4.90	0.90	3.63	2.78	2.47
15	3.95	2.01	5.94	1.10	26.07	3.16	3.00
16	3.33	1.69	5.01	0.92	19.19	3.34	2.52
17	2.87	1.46	4.32	0.80	23.11	2.63	2.18
18	3.82	1.95	5.75	1.06	16.56	2.95	2.90
19	2.49	1.27	3.75	0.69	15.02	1.41	1.89
20	3.54	1.80	5.32	0.98	14.71	2.96	2.68

Table 3.4: *PD population parameters - Urine output*

Subject	a [mL/h]	b	c [mg/h]	d [L/h]
0	44.70	1.63	4.45	0.54
1	37.74	1.63	3.93	0.39
2	53.19	1.69	4.57	0.41
3	45.44	1.60	4.11	0.63
4	56.56	1.63	3.28	0.44
5	48.82	1.61	2.76	0.63
6	47.98	1.67	3.55	0.56
7	45.01	1.64	3.16	0.45
8	42.89	1.61	5.36	0.63
9	43.71	1.58	3.88	0.66
10	31.50	1.54	5.45	0.7
11	41.00	1.63	5.43	0.33
12	27.02	1.69	3.97	0.45
13	48.83	1.74	1.51	0.56
14	41.65	1.66	5.59	0.4
15	20.47	1.59	4.74	0.69
16	38.71	1.63	4.72	0.54
17	55.67	1.66	7.36	0.49
18	61.14	1.58	2.57	0.56
19	43.18	1.64	6.82	0.47
20	52.05	1.60	2.97	0.63

Chapter 4

Mathematical Models of Renal Activity

The pharmacology of furosemide is only the first step for a complete model to describes the process of decongestion. The PKPD model help us describing the organism's response to the drug, but it does not give a faithful representation of the renal function as a whole, especially when no diuretic is administered.

Therefore, we focused on finding and evaluating mathematical models that accurately described the renal system. Unfortunately, because of the severe physiological complexity of the system itself, there are not many works that provide a full and working model that would satisfy our needs.
In particular, most of the attempts recorded in literature were written in the '70s and '80s, and only a few considered the *human* renal system. In addition to that, we needed a model that was not centred around the fluidodynamics and mechanical resistance of the blood and urine vessels, but rather could predict urine excretion based on the water inflow and the patient's current level of hydration.

In the end, we selected two models that could answer our needs, and we focused our analysis on the feasibility of adapting them to our work.

4.1 Uttamsingh, 1985

The first model, by Uttmasingh[26], is the most complex and the older of the two. It is a complex body-fluid system model that gathers in a single model most of the key equations that had been used to describe different aspects of renal function up until 1985.

Uttmasingh's model is comprised of four interrelated physiological subsystem models that represent hormonal and cardiovascular control and regulation of renal action for both water, sodium, and potassium distribution.

Each of the four subsystems models an aspect of the physiological processes involved in renal activity.

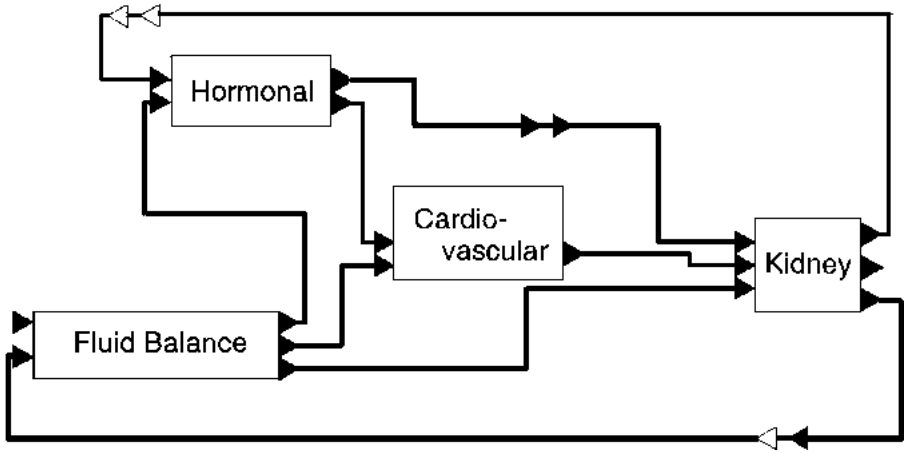

Figure 4.1: *Schematic representation of Uttamsingh's model*

In 1997, Cloutman[27] revisited the model simplifying the cardiovascular and the fluid balance blocks. We will review his modifications in the corresponding sections.

4.1.1 Kidney System

The kidney subsystem can be further divided into three blocks, corresponding to the three sections of the tubule: proximal tubule, loop of Henle, and distal tubule.
The equations describe the entering flows and reabsorption rates of water and sodium through each section of the tubule.

Proximal tubule (PT) equations:

$$F_{Na} = GFR \cdot \frac{Na_P}{1000} \tag{4.1}$$

$$GTB = 5.815 - 0.0357 \cdot Na_P \tag{4.2}$$

$$R_{Na,PT} = GTB \cdot F_{Na} \tag{4.3}$$

$$R_{W,PT} = GTB \cdot GFR \tag{4.4}$$

where $R_{Na,PT}$ and $R_{W,PT}$ are the reabsorption rates of sodium and water respectively, along the proximal tubule; Na_P is the plasma concentration of sodium; F_{Na} is the filtration rate of sodium into the proximal tubule; and GTB is the glomerular-tubular balance, which is the linear relationship between proximal tubular reabsorption and glomerular filtrarion rate GFR, and describes the phenomenon whereby if the GFR spontaneously increases, the rate of water and solute resorption in the tubule proportionally increases, thus maintaining the same fraction of the filtered load being resorbed[28, 29].
The GFR in this model is estimated through a linear piecewise function of the arterial pressure P_A (see Appendix A.1).

Loop of Henle (LH) equations:

$$J_{Na,LH} = F_{Na} - R_{Na,PT} \tag{4.5}$$
$$J_{W,LH} = GFR - R_{W,PT} \tag{4.6}$$
$$R_{W,LH} = 0.65 \cdot J_{W,LH} - 0.01 J_{W,LH}^2 \tag{4.7}$$
$$R_{Na,LH} = 0.8 J_{Na,LH} \tag{4.8}$$

where, $J_{W,LH}$ and $J_{Na,LH}$ represent the entering flows of water and sodium, respectively, into the loop of Henle.
Distal tubule (DT) equations:

$$J_{Na,DT} = J_{Na,LH} - R_{Na,LH} \tag{4.9}$$
$$J_{W,DT} = J_{W,LH} - R_{W,LH} \tag{4.10}$$
$$R_{W,DT} = B_{W,DT} \cdot J_{W,DT} \tag{4.11}$$

where $B_{W,DT}$ is the fraction of water load reabsorbed in the distal tubule. It is a quantity dependent on the concentration of the anti-diuretic hormone (ADH), and it is approximated by a piecewise function. $J_{W,DT}$, $J_{Na,DT}$, $R_{W,DT}$, and $R_{Na,DT}$ follow the same nomenclature as before.

The outputs of interest of the system are the urine, sodium, and potassium outflows:

$$J_U = J_{W,DT} - R_{W,DT} \tag{4.12}$$
$$J_N a = J_{Na,DT} - R_{Na,DT} \tag{4.13}$$
$$J_K = 0.107 K_P - 0.505 + U_{K,ALD} \tag{4.14}$$

where $U_{K,ALD}$ is the excretion rate of potassium due to aldosterone (ALD). The swept responses of GFR, $B_{W,DT}$, $R_{Na,DT}/J_{Na,DT}$, and $U_{K,ALD}$ are shown in Figure 4.2. The piecewise functions that describe each quantity are fully reported in the Appendix A.

As we said, the kidney subsystem is divided into three sections, but since we are more interested in the overall product of the filtration-reabsorption process, instead of what happens in each section specifically, the equations can be rewritten to allow a clearer picture of the interdependencies and the effects of the different variables.

$$J_U = (1 - f(ADH)) \cdot (0.35 GFR(0.036 Na_P - 4.8) + 0.01 GFR^2 \cdot (0.036 Na_P)^2) \tag{4.15}$$

$$J_{Na} = J_{Na,DT} - R_{Na,DT} = J_{Na,DT} \cdot (1 - f(ALD)) \tag{4.16}$$
$$= 0.2GFR \cdot \frac{Na_P}{100} \cdot (0.036Na_P - 4.8)(1 - f(ALD))$$
$$J_K = 0.1K_P - 0.5 + f_K(ALD) \tag{4.17}$$

The equations themselves underline the effects of the hormones on the outputs of the system:

- J_U is reduced when there is a higher concentration of ADH, as the anti-diuretic hormone promotes water retention;
- J_{Na} is lower when aldosterone is released in the organism, which is mirrored by an increase in the excretion of potassium, since aldosterone promotes sodium reabsorption on an almost one-to-one ration with potassium excretion.

We could further underline the major dependencies of each output:

$$J_U = f(V_{EX}, Na_P, ADH) \tag{4.18}$$
$$J_{Na} = f(V_{EX}, Na_P, ALD) \tag{4.19}$$
$$J_K = f(K_P, ALD) \tag{4.20}$$

This shows how the urine and salt outflow are directly dependent on the extracellular volume and the sodium concentration in plasma and that both quantities are controlled by the presence of a hormone, ADH in the case of urine, and aldosterone in the case of salt. The excretion of potassium is dependent on the potassium plasma concentration as well as the quantity of aldosterone present.

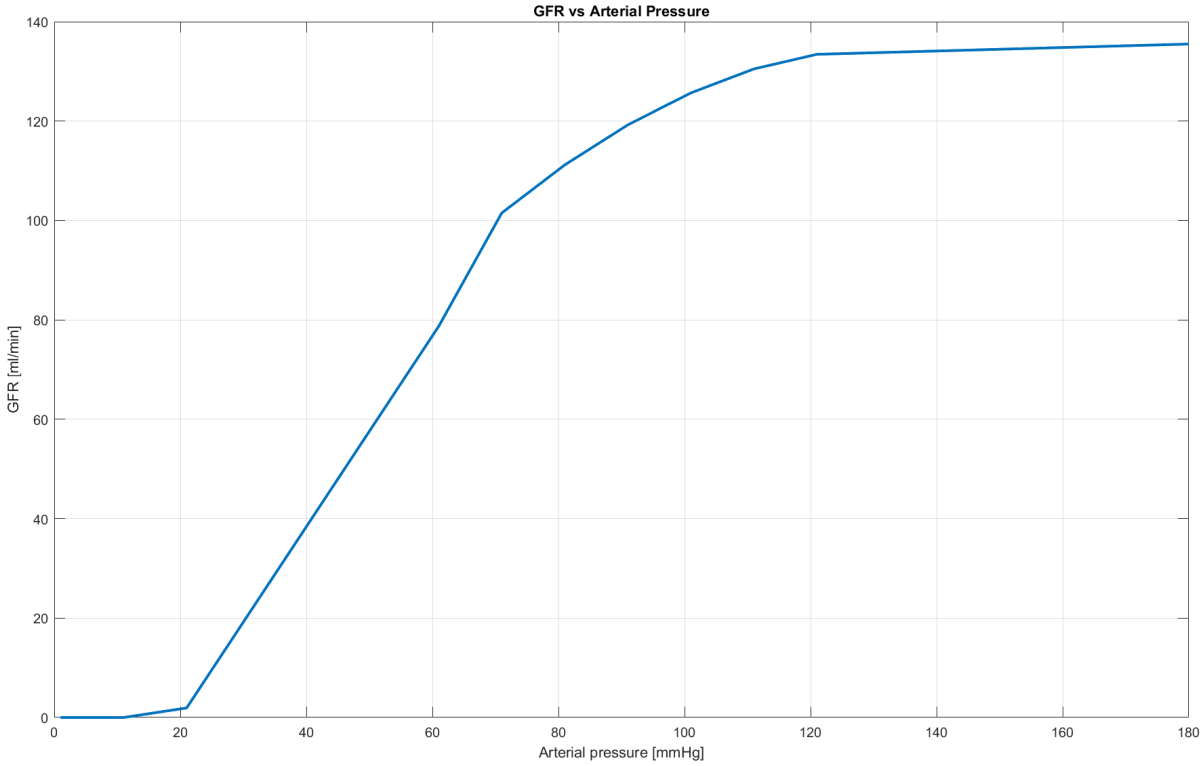

(a) *GFR vs Arterial Pressure*

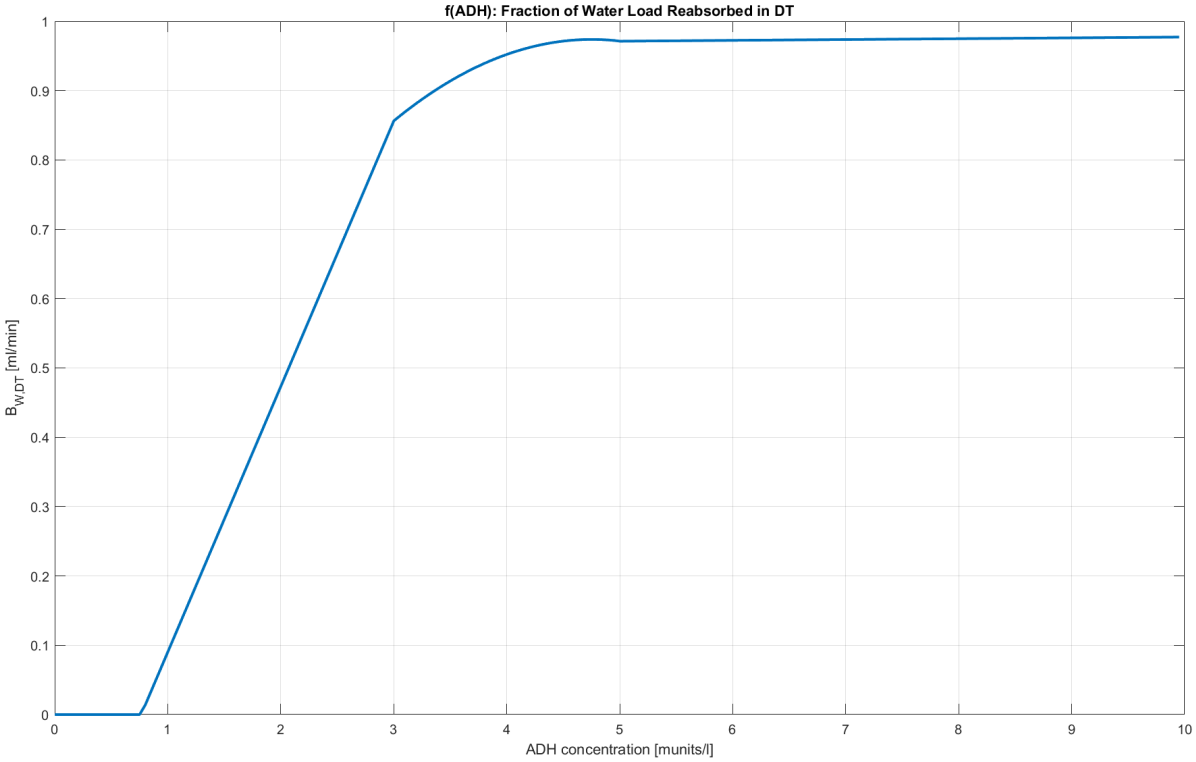

(b) *Fraction of water load reabsorbed in the distal tubule, function of ADH.*

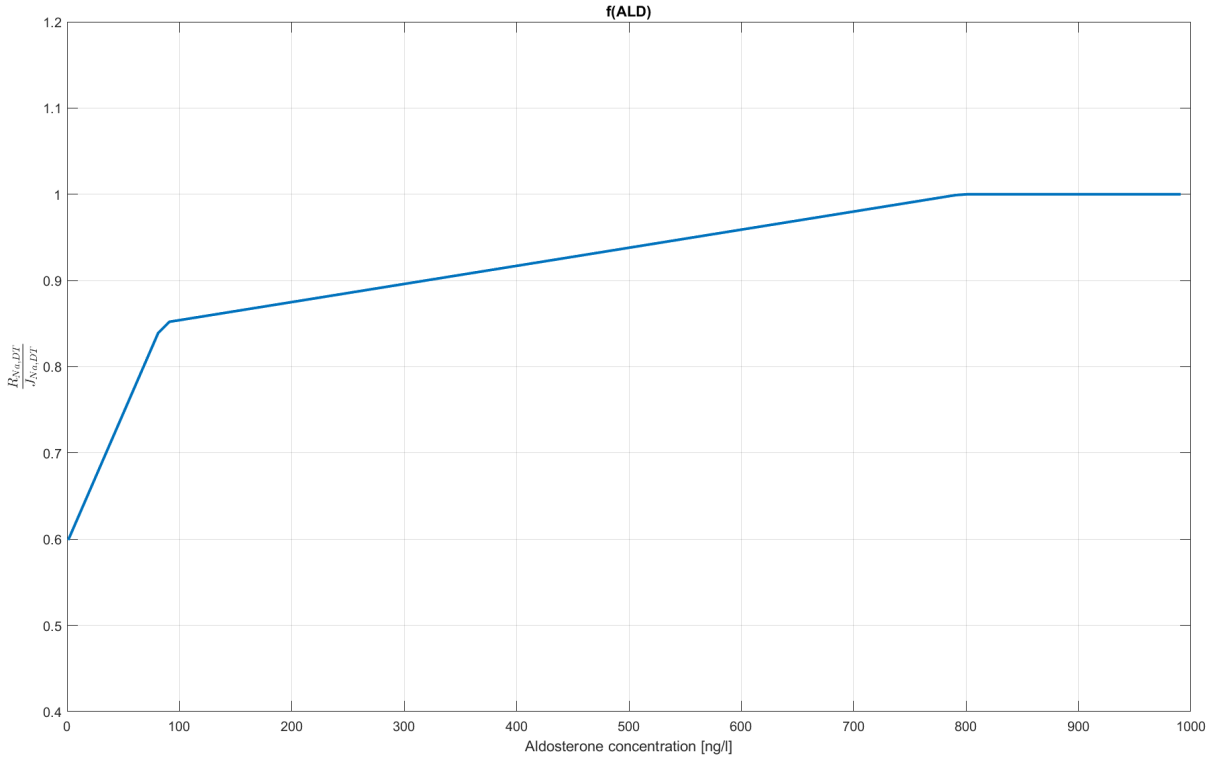

(c) Reabsorbed sodium in the distal tubule over the rate of flow of sodium into the distal tubule, function of ALD

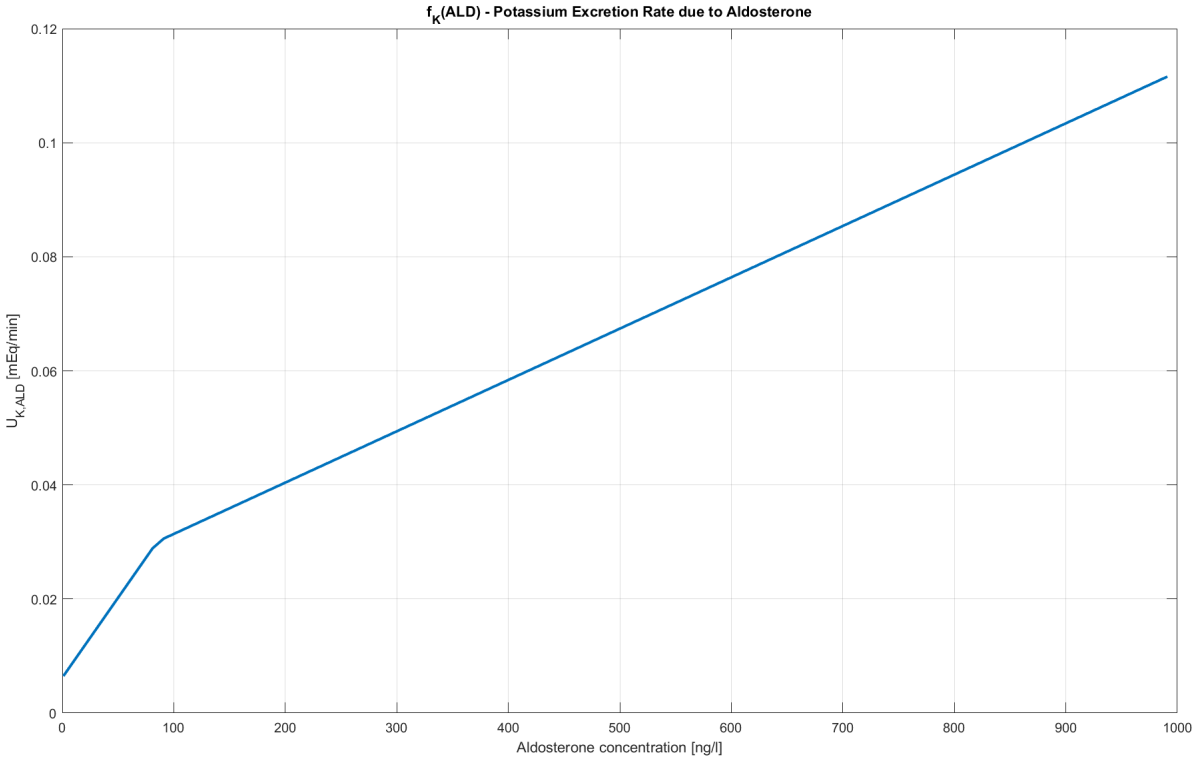

(d) $U_{K,ALD}$*. Note: this is the same quantity* $f_{K,ALD}$ *from Eq 4.17*

Figure 4.2: *Generated graphs of the piecewise functions in the Kidney block. Done with MATLAB®.*

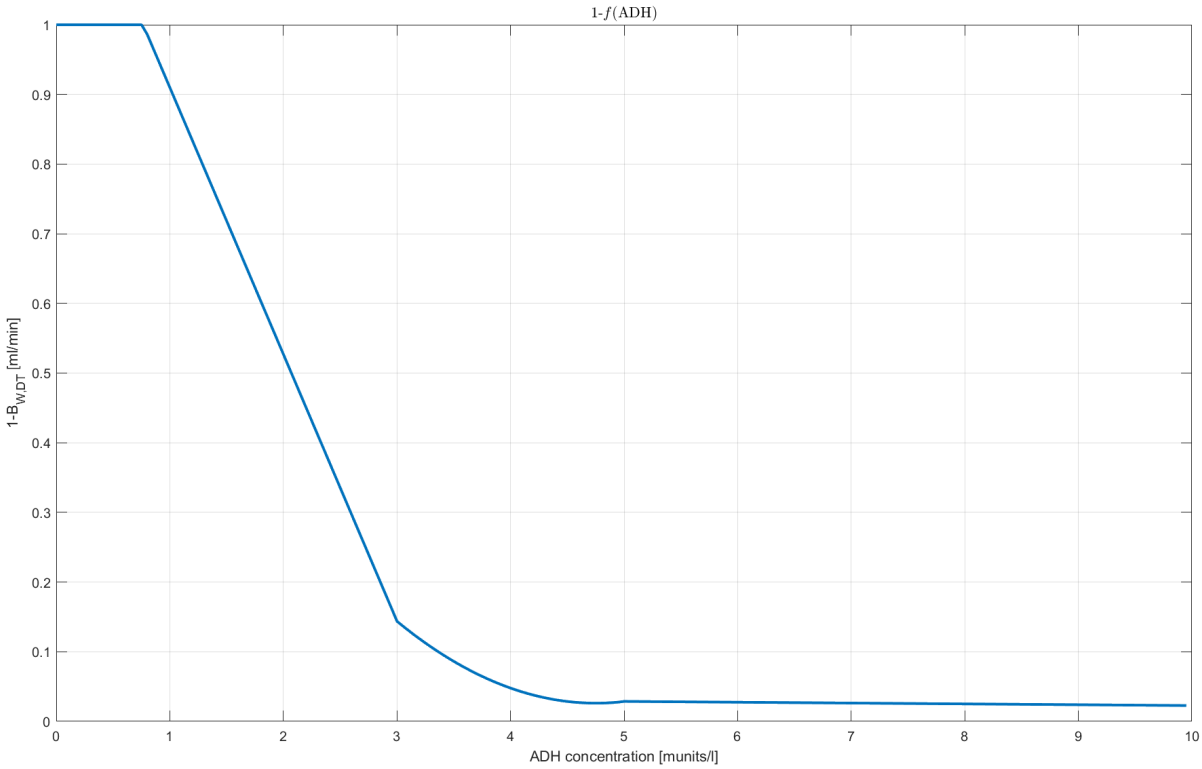

(e) $1 - f(ADH)$ *from Eq. 4.15*

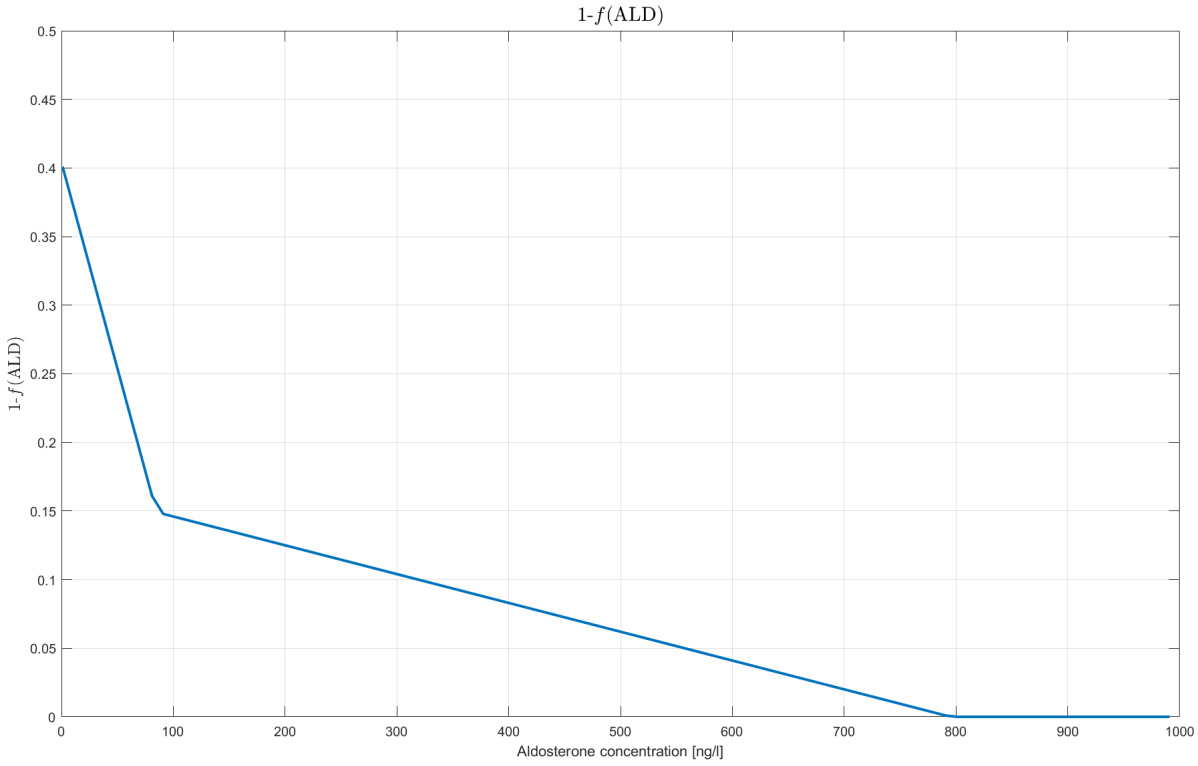

(f) $1 - f(ALD)$ *from Eq. 4.16*

Figure 4.3: *Generated graphs of* $1 - f(ADH)$ *and* $1 - f(ALD)$ *from 4.15 and 4.16. Note that* $f(ADH) = B_{W,DT}$ *and* $f(ALD) = R_{Na,DT}/J_{Na,DT}$. *Done with MATLAB®.*

4.1.2 Hormonal System

The hormone subsystem tracks the plasma concentrations of four main hormones involved in renal activity: the anti-diuretic hormone (ADH or vasopressin), renin (R), angiotensin II (A), and aldosterone (ALD).

$$\frac{dADH}{dt} = \frac{ADHS - ADH \cdot Cl_{ADH}}{P} \tag{4.21}$$

$$\begin{aligned} \frac{dR}{dt} &= \frac{RS - 0.135R}{P} \\ &= \frac{0.0163 - 0.0093J_{Na,DT} - 0.135R}{P} \end{aligned} \tag{4.22}$$

$$\begin{aligned} \frac{dA}{dt} &= \frac{AS - 4.04A}{P} \\ &= \frac{583.3R \cdot P - 4.04A}{P} \end{aligned} \tag{4.23}$$

$$\frac{dALD}{dt} = \left(\frac{3.0f_(ANGII) + 21.64K_P - 55.5}{4.0} - 0.62ALD\right) \cdot \frac{1}{P} \tag{4.24}$$

P is the plasma volume which is approximately 0.6 times the blood volume V_B. $ADHS$ is the release rate of ADH and it is dependent on the variation of V_{EX}; Cl_{ADH} is the clearance rate of ADH; $f(ANGII)$ is the function representing the release rate of aldosterone, dependent on the concentration of angiotensin II. These three quantities are approximated by piecewise functions, their swept responses are shown in Figure 4.4. The piecewise functions that describe each quantity are fully reported in the Appendix A.

These equations show that all the hormone concentrations are dependent on the plasma volume and therefore, as we will see in Section 4.1.3, they are dependent on the extracellular fluid volume.

The interdependence of the RAAS system is clear as well, with the concentration of renin influencing the formation of angiotensin (AS), which in turn determines the excretion of aldosterone through the term $f(ANGII)$, which represents the release rate of aldosterone due to the concentration of angiotensin II in plasma.

Renin release RS is also dependent on the concentration of sodium in plasma, through the quantity $J_{Na,DT}$. Since aldosterone is ultimately influenced by renin, as we have just seen, ALD is actually a function of both potassium and sodium concentrations.

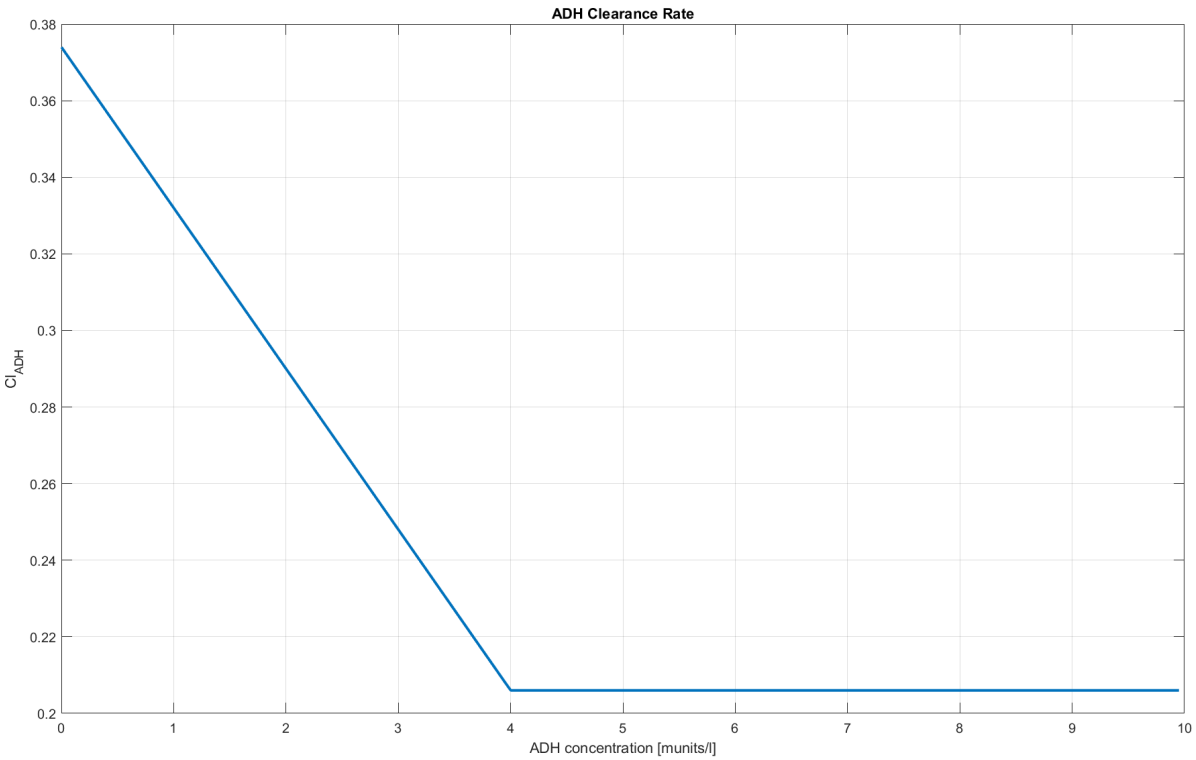

(a) *ADH Clearance rate*

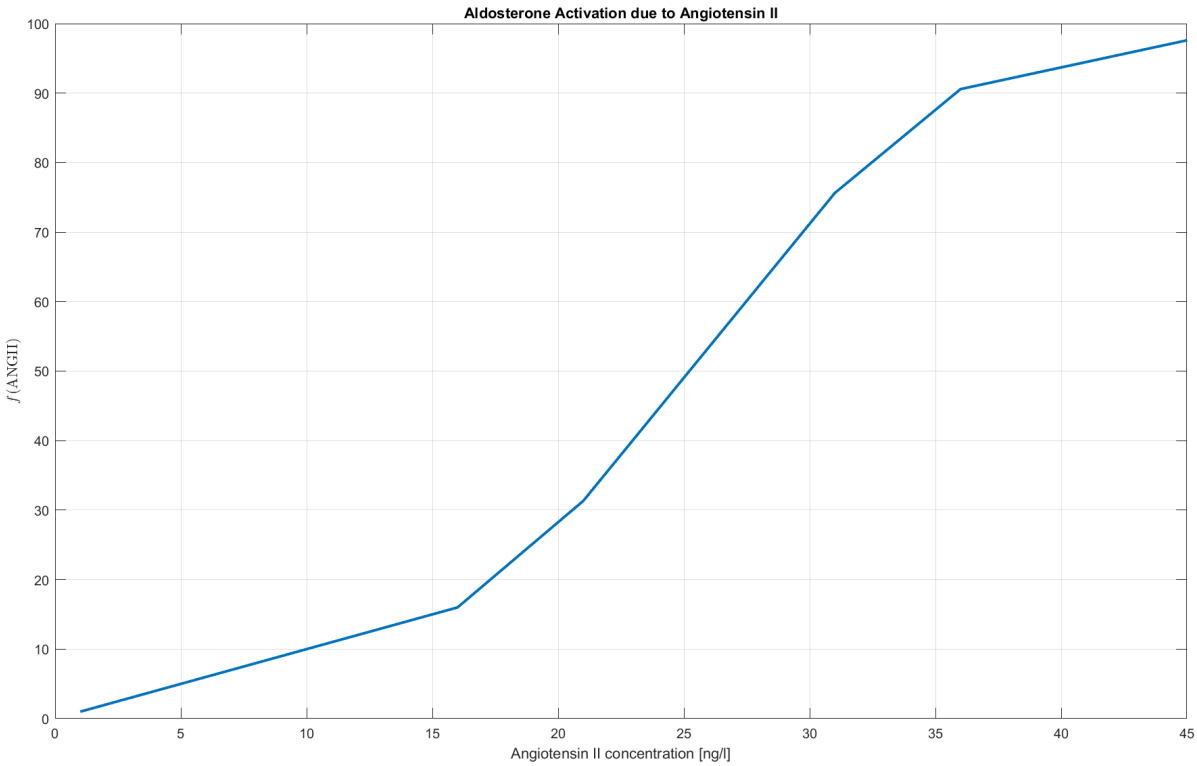

(b) *$f(ANGII)$ from Eq. 4.24*

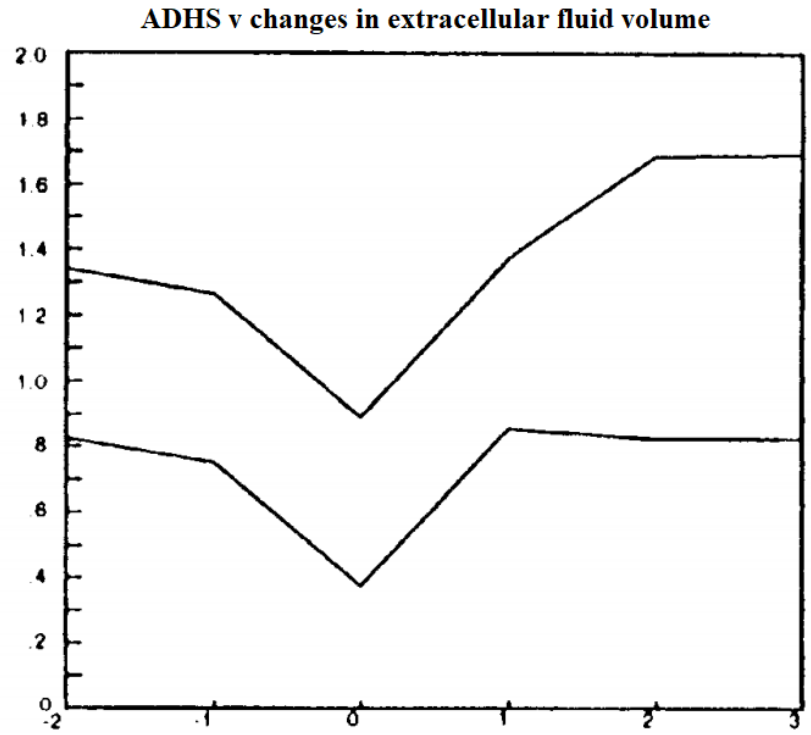

(c) ADH release rate

Figure 4.4: *Generated graphs of the piecewise functions in the Hormone block. 4.4a and 4.4b were done with MATLAB®. 4.4c is taken directly from [27] as we have not been able to replicated the ADHS function in MATLAB® because of its complexity.*

4.1.3 Cardiovascular System

In Uttmasingh's model, the cardiovascular block is complex and takes into consideration several quantities that are difficult to estimate. A kidney simulator based on Uttmasingh's model by Cloutman[27], though, gives us a simplified version that can be acceptable for our purposes. Uttmasingh's original version is described in depth in Appendix A.

The most important output of this block is the arterial pressure P_A, which is ultimately dependent on the extracellular fluid volume V_{EX} through the blood volume V_B and the mean systemic pressure P_{MS}.

Cloutman's equations for this block thus are:

$$P = 0.6 \cdot V_B \tag{4.25}$$

$$V_B = 0.33 \cdot V_{EX} \tag{4.26}$$

$$P_{MS} = 3.5(V_B - 3) \tag{4.27}$$

$$P_A = \frac{P_{MS}}{0.07} \tag{4.28}$$

4.1.4 Fluid Balance System

Lastly, the fluid balance block describes the rates of change of extracellular fluid volume, extracellular sodium, and extracellular potassium in terms of their respective rates of ingested and excreted quantities.
This is another block that was simplified by Cloutman in his model, where the only significant equations reported are

$$\frac{dV_{EX}}{dt} = J_{W,ingested} - J_U \tag{4.29}$$
$$\frac{dNa_{EX}}{dt} = J_{Na,ingested} - J_{Na} \tag{4.30}$$
$$\frac{dK_{EX}}{dt} = J_{K,ingested} - J_K \tag{4.31}$$

The simplification by Cloutman is in regards to the quantity V_{EX}. Cloutman considers the variation of external fluid volume as the direct difference between the rate at which ingested water passes through the gut and the rate of urine formation, but this does not take into account that the water ingested can also be deviated to intracellular spaces.
Uttmasingh's model is more accurate on this point, by considering the water compartment W of the whole body partitioned into an extracellular V_{EX} and an intracellular V_{IN} space. The actual fluid balance is thus

$$\frac{dW}{dt} = J_{W,ingested} - J_U \tag{4.32}$$

By keeping into consideration the intracellular compartment, though, we must also keep track of the rates of change of sodium Na_{IN} and potassium K_{IN} in the intracellular compartment as well. In Uttmasingh's model, these are considered constants in a dynamic balance.
The electrolyte concentrations in both compartments then become

$$Na_P = \frac{Na_{EX}}{V_{EX}} \qquad Na_I = \frac{Na_{IN}}{V_{IN}}$$
$$K_P = \frac{K_{EX}}{V_{EX}} \qquad K_I = \frac{K_{IN}}{V_{IN}}$$

Which ensues that the equating osmolities are

$$\frac{Na_{EX} + K_{EX} + c_{EX}}{E} = \frac{Na_{In} + K_{IN} + c_{IN}}{V_{IN}}$$

where c_{EX} and c_{IN} are constants representing the osmotic effect of the remaining body fluid compartments not modelled here.

By rewriting

$$T_{EX} = Na_{EX} + K_{EX} + c_{EX} \tag{4.33}$$

$$T_{IN} = Na_{In} + K_{IN} + c_{IN} \tag{4.34}$$

we can finally determine that

$$V_{EX} = W(1 + \frac{T_{IN}}{T_{EX}})^{-1} \tag{4.35}$$

and

$$V_{IN} = W(1 + \frac{T_{EX}}{T_{IN}})^{-1} \tag{4.36}$$

Unfortunately, Uttamsingh's model does not provide a parametric estimation of the quantities concerning the intracellular compartment, only average values for the constants, without a variability measure.

4.1.5 Limitations

Uttmansingh's model is a very interesting tool especially since it takes into consideration that each section of the nephron has different reabsorption capabilities, which is interesting because we know exactly which portion of the nephron is affected by furosemide. Unfortunately though, the model is fitted to healthy subjects, and we don't know if and how the equation's parameters change in the presence of congestive heart failure.

More importantly, though, while we know that the site of action of furosemide is the loop of Henle, where the drug acts by inhibiting some electrolyte transporters, we have no way of knowing, without experimentation, how to account for its presence in this model. Furthermore, the PKPD model of furosemide does not account for the excretion of potassium, which is reasonably bound to change in response to the drug, as one of the most common side effects of loop diuretic therapy is hypokalemia.

Additionally, to compute the plasma concentration of ADH we need to also compute the activation of ADH, $ADHS$, and those equations include a hidden variable, the plasma osmolarity, which is not otherwise described within the model. Its estimation is not entirely straightforward, and it requires additional information, such as glucose levels, which would further complicate the model.

4.2 Gyenge's Model, 2003

A much more simplified mathematical model of the kidney was proposed by Gyenge et al. in 2003[30] as part of a bigger model for the transport of fluids and solutes in the

body[31]. Figure 4.5 shows the schematic representation of the kidney model as well as its relationship to the overall whole-body fluide and solute exchange.

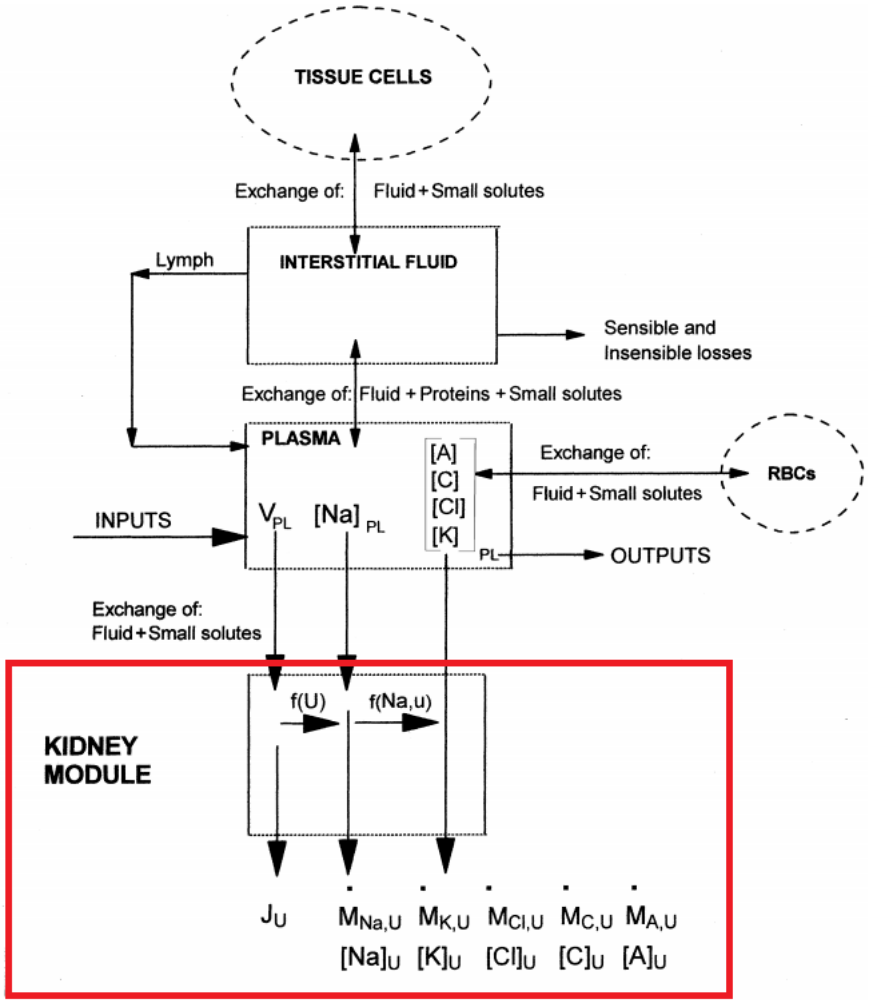

Figure 4.5: *Schematic representation of the kidney model (red) as well as its relation to the overall whole body-fluid model by Gyenge et al.[30, 31]*

The renal module developed by Gyenge assumes first-order, negative feedback response to changes in plasma volume and plasma sodium content from the normal physiological conditions. Hormonal activity is not explicitly formulated, and the excretion of electrolytes other than sodium is proportional to the excretion of sodium itself.

The model describes two main phenomena: fluid excretion and electrolyte excretion.

4.2.1 Fluid Excretion

As we said, the fluid excretion equation assumes a first-order negative-feedback response to the variation of the plasma volume P from its normal value P_{NC}.

The urinary output rate J_U [mL h^{-1}] therefore is

$$J_U = k_U \cdot \frac{P - P_{NC}}{P} + J_{U,NC} \tag{4.37}$$

$J_{U,NC}$ is the normal urinary output rate, which is about 60ml h^{-1} for an average 70-kg human.
k_u [mL h^{-1}] is a flux rate that has been estimated to change in relation to if the subject is in a condition of high hydration ($P \geq P_{NC}$) or dehydration ($P < P_{NC}$). Therefore,

$$k_U = \begin{cases} k_U^D & \text{if } P < P_{NC} \\ k_U^E & \text{if } P \geq P_{NC} \end{cases} \tag{4.38}$$

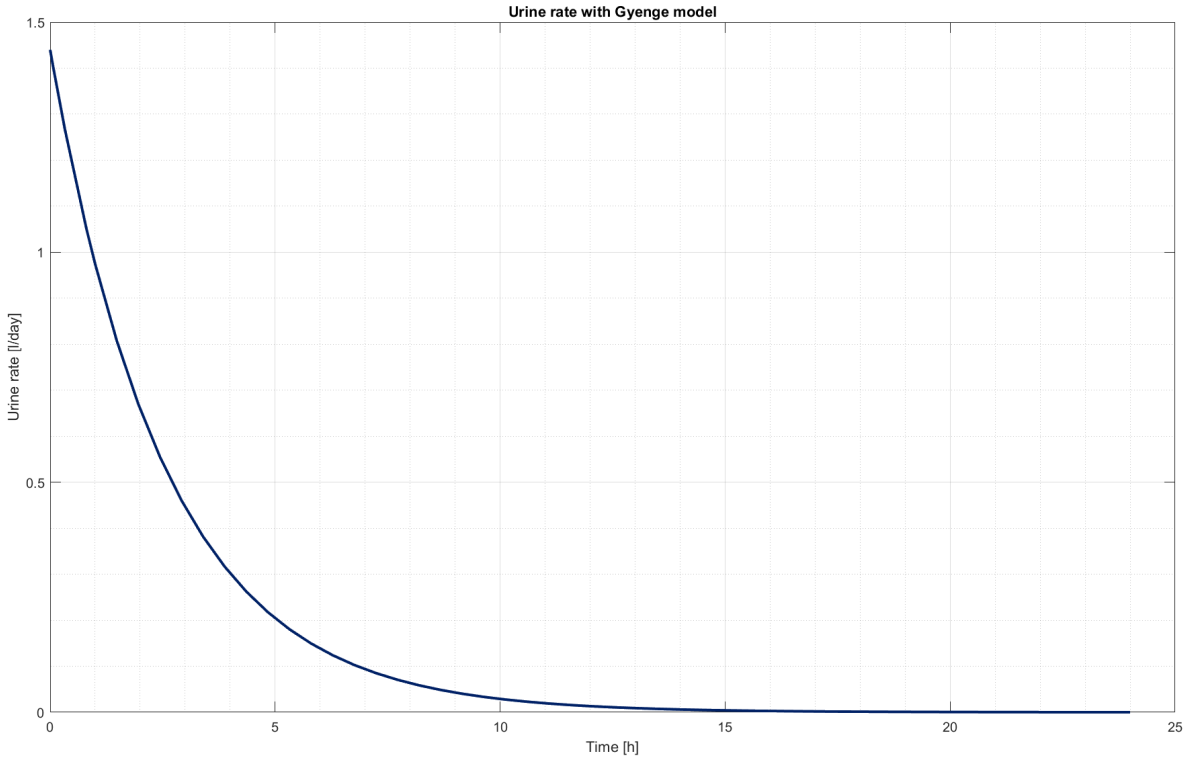

(a) *Urine excretion rate*

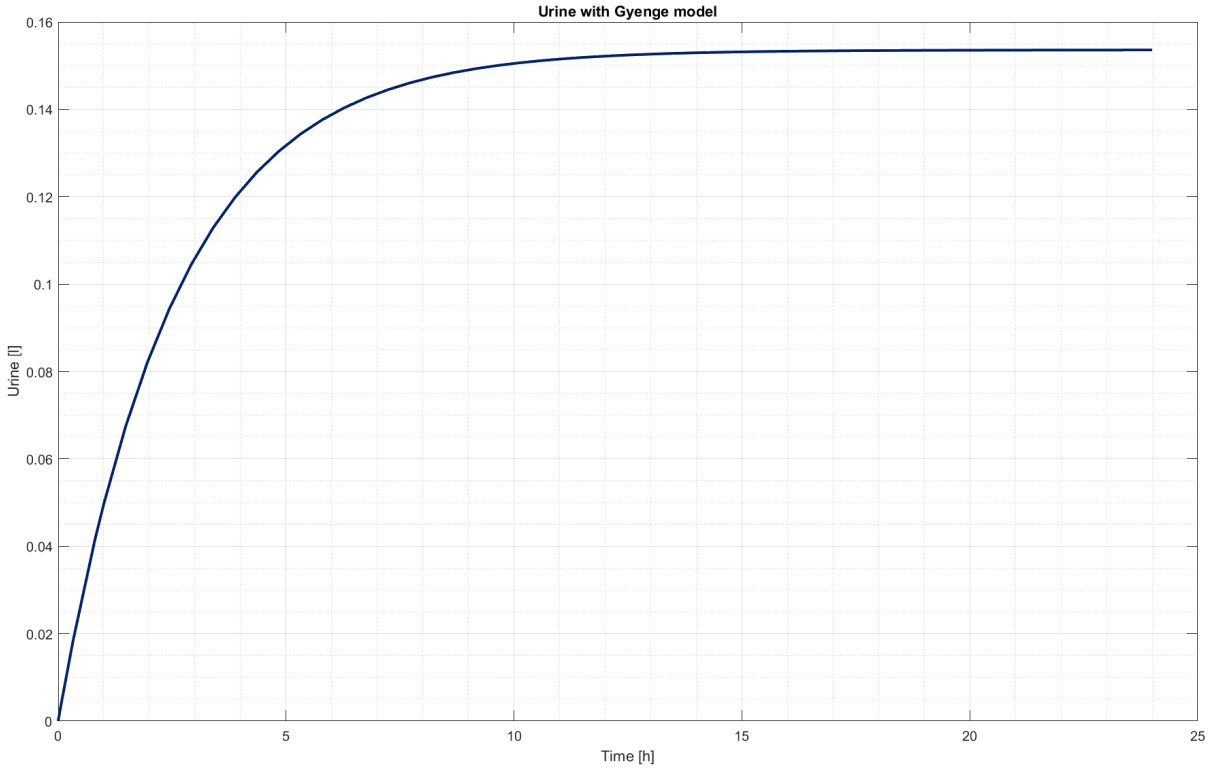

(b) Cumulative urine excretion

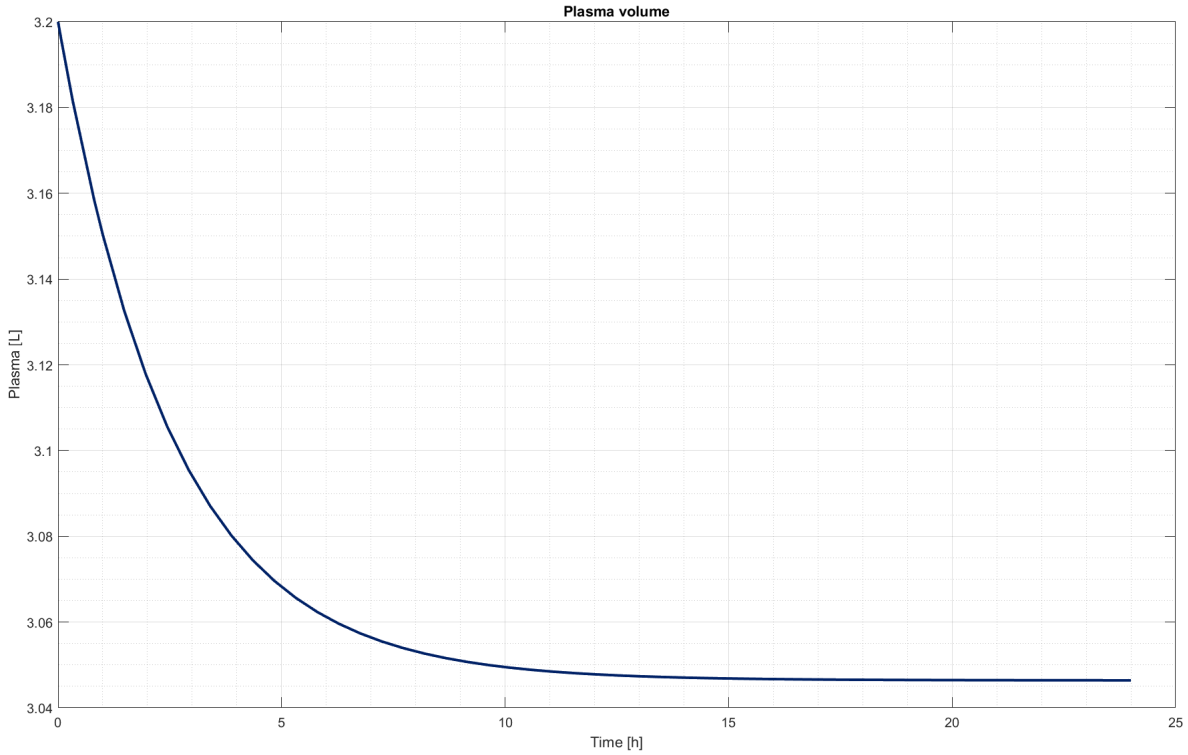

(c) Plasma volume

Figure 4.6: *Output of Gyenge's fluid block, considering a healthy patient with starting plasma volume of 3.2L*

4.2.2 Sodium excretion

Assuming that renal clearance of sodium Cl_{Na} is proportional to the variation in sodium concentration in plasma from its normal value $Cl_{Na,NC}$,

$$Cl_{Na} = \left(k_{Na} \cdot \frac{Na_P - Na_{P,NC}}{Na_{P,NC}} + Cl_{Na,NC} \right) \cdot F(U) \tag{4.39}$$

where k_{Na} (ml h^{-1}) is a proportionality constant.
$F(U)$ is an empiric factor that couples sodium excretion with the urinary flow rate:

$$F(U) = \begin{cases} \frac{J_U}{J_{U,NC}} & \text{if } Na_P < Na^T_{P,NC} \\ 1 & \text{if } Na_P \geq Na^T_{P,NC} \end{cases} \tag{4.40}$$

where $Na^T_{P,NC}$ is the threshold sodium concentration in plasma, or the maximal value of normal physiological range of plasma sodium concentration.

Since sodium clearance can also be written as

$$Cl_{Na} = Na_U \cdot \frac{J_U}{Na_P} \tag{4.41}$$

we can compute the sodium excretion rate J_{Na} using Equation 4.39

$$\begin{aligned} J_{Na} &= Na_U \cdot J_U \\ &= \left(k_{Na} \cdot \frac{Na_P}{Na_{P,NC}} (Na_P - Na_{P,NC}) + Cl_{Na,NC} \cdot Na_P \right) \cdot F(U) \end{aligned} \tag{4.42}$$

4.2.3 Limitations

As we have seen, Gyenge's model is much more simplified than Cloutman's, since it doesn't take into direct consideration the action of the several hormones involved in renal activity, and it reduces the interdependencies between plasma volume and sodium concentration to a single control action performed by the urine excretion on the sodium excretion.
Furthermore, as was the case with the previous model, we don't have any information on how the injection of furosemide can affect the equations that make up the model.

4.3 Model Comparison

While the two models are very different, they both unfortunately present two very important limitations to our purposes, namely that they are fitted to the physiological behaviour of healthy subjects, and that they don't provide for the addition of the diuretic effects on the system promoted by furosemide.

The kidney is a very complicated biological machine, with plenty of interconnected mechanisms that respond to the minimal change in the organism's physiological balance in order to ensure and maintain homeostasis. In the case of CHF, the equilibrium point is offset and renal activity can be markedly impaired compared to that of a healthy subject. This means that models of a *healthy* renal system are not accurate for our purposes.

We also know that because of the complexity of the homeostasis mechanisms, the effects of furosemide can differ widely between patients and there is not a mathematical model of the kidney that keeps it into account, therefore it is challenging to effectively merge the physiological model with the furosemide PKPD model described in Chapter 3.

We thoroughly examined both renal mathematical models and we asked our clinical partners for their opinion on them, in order to choose the one best suited to our needs. It is important to note that our decision was influenced by several factors, and we were affected most of all by the lack of one crucial ingredient: time.

In the end, we decided to discard Uttamsingh's model, because, while on paper it seems to be the most complete model of the two, its complexity makes it much more difficult to adapt on a short notice. In addition to that, as explained in Section 4.1.5, there is one parameter, plasma osmolarity, that is required by the model but not estimated by it, and which would require another thorough round of research to be able to estimate it properly, which we could not afford doing.

Therefore, we settled on adapting Gyenge's model to our purposes by trying to chain its inputs to the PKPD outputs. Chapter 5 thoroughly explains Our process to achieve that.

Chapter 5

Integrating the Models

5.1 Integration with Gyenge's model

Once we selected the renal activity model to implement, we had to integrate it with the PKPD model of the drug.

As explained in Chapter 3, the pharamcodynamics of furosemide are modelled by Equation 3.2

$$Y = \frac{a - d}{1 + (\frac{X}{c})^b} + d$$

where the output Y is the urinary excretion rate due to the action of furosemide.

As seen in Equation 4.37, in Gyenge's model the final rate of urine production is the sum of the average urine flow and an error directly dependent on the changes in plasma volume from a physiological set point.

$$J_U = k_U \cdot \frac{P - P_{NC}}{P_{NC}} + J_{U,NC}$$

Therefore, to link the two models together, we swapped the average urine flow $J_{U,NC}$ used by Gyenge with the output of the furosemide model, $J(F) = Y$.

$$J_U = k_U \cdot \frac{P - P_{NC}}{P_{NC}} + J(F) \tag{5.1}$$

We also decided to consider a simplified version of Gyenge's model, discarding the dependency on k_U due to the state of hydration of the subject by keeping only the coefficient linked to a higher hydration status.

5.2 Disturbance

Even when patients are congested, they still drink and eat regularly, albeit usually with a controlled low-sodium diet.The model introduced so far does not account for this inflow.

Drinking, sweating and water loss due to respiration are the most common disturbances that can act on the system.

Respiratory water loss is negligible, especially if we consider a temperature controlled environment, and a patient who is not under physical exertion, which is a sensible assumption for an hospedalised patient. By considering a controlled environment, we can also consider sweating a negligible disturbance, as it would also be quite difficult to represent through a mathematical model, because of the high variability in sweat production due to external temperature, activity levels, and the overall characteristics of the subject.

On the other hand, drinking can be approximated by a more intuitive model, therefore, for our model, we only considered the disturbance caused by the subject drinking a token amount of water every few hours.

We considered a very simple tri-compartmental model, representing the stomach, intestines, and plasma (Fig 5.1).

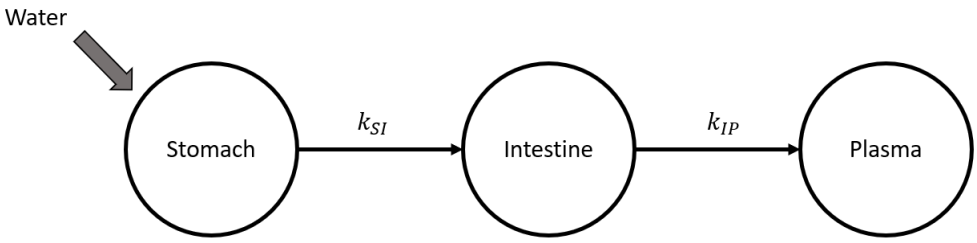

Figure 5.1: *Drinking compartmental model*

In this way, the won't always be an outflow from the plasma compartment, since a certain amount of fluid will replenish the plasma volume after the patient drinks some water.

5.3 Complete Model

The final version of the model we want to implement therefore is comprised of three blocks (Fig. 5.2):

- Furosemide: The PKPD model which computes the effect on the urinary flow forced by the drug;

- Kidneys: The block that describes the kidneys' response to changes in plasma volume, and outputs the current plasma volume and urinary excretion rate;

- Drinking: The disturbance block that allows for plasma replenishing after the subject drinks water.

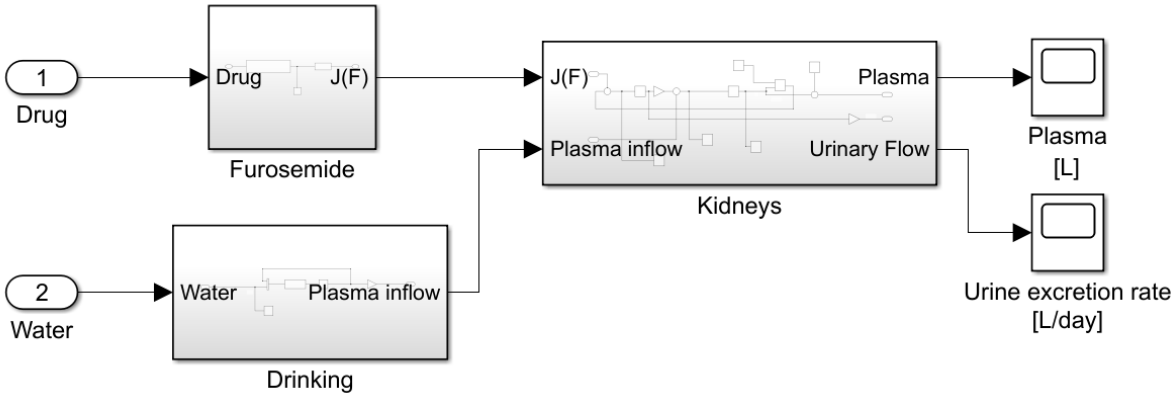

Figure 5.2: *Simulink® final model scheme*

We had to discard the modelling of salt excretion, because after consulting with clinical experts it was deemed too inaccurate and correcting it would have required more literature research and unfortunately our timetable didn't allow for that.

Figure 5.3 shows the responses of the system in different conditions:

- **Fig. 5.3a** shows the system response without any diuretic and with a patient that does not drink.

- **Fig. 5.3b** shows the system response without any diuretic, but with an intake of 0.5L of water every 9 hours.

- **Fig. 5.4c** shows the system response when there is not any water intake, but a dose of 40mg of furosemide is administered every 6 hours.

- **Fig. 5.4d** shows the system response when the patient drinks 0.5L of water every 9 hours and is administered 40mg of furosemide every 6 hours.

Figure 5.3: *Simulation of the system under different conditions*

(a) *Plasma output for the average patient with no furosemide.*

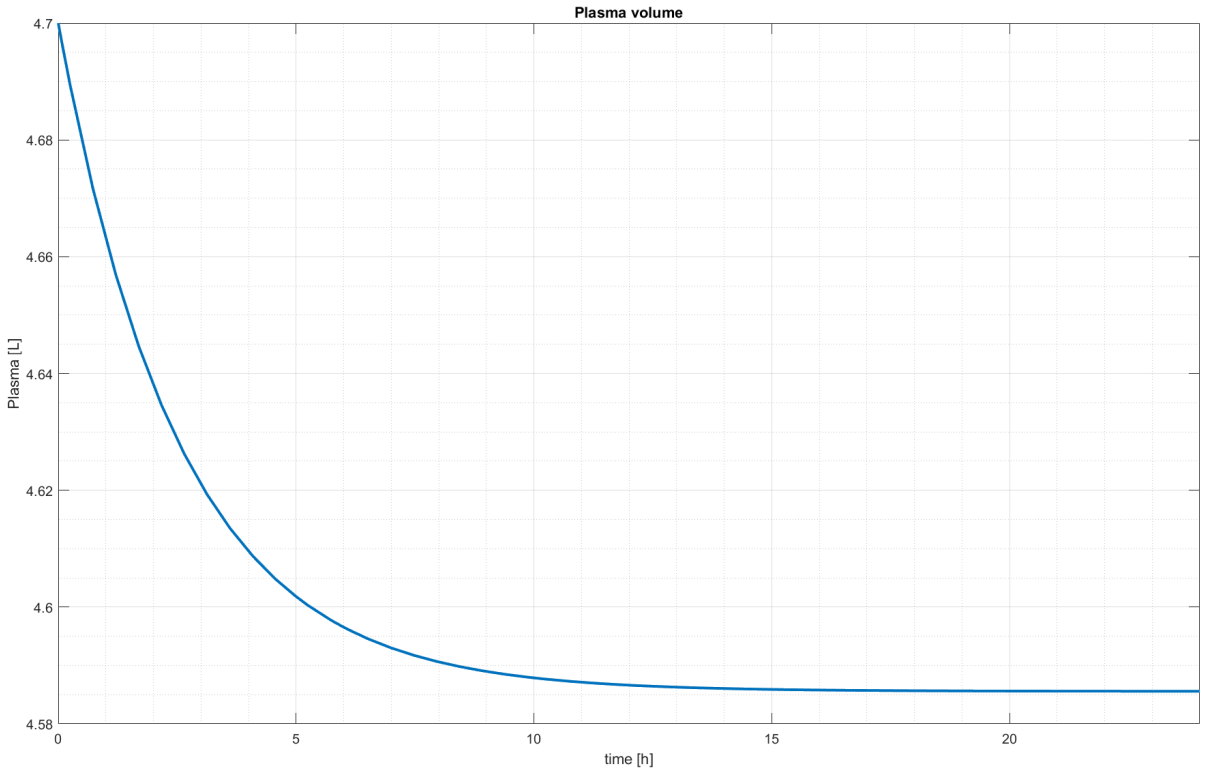

(b) *Plasma output for the hydrated average patient without diuretic therapy.*

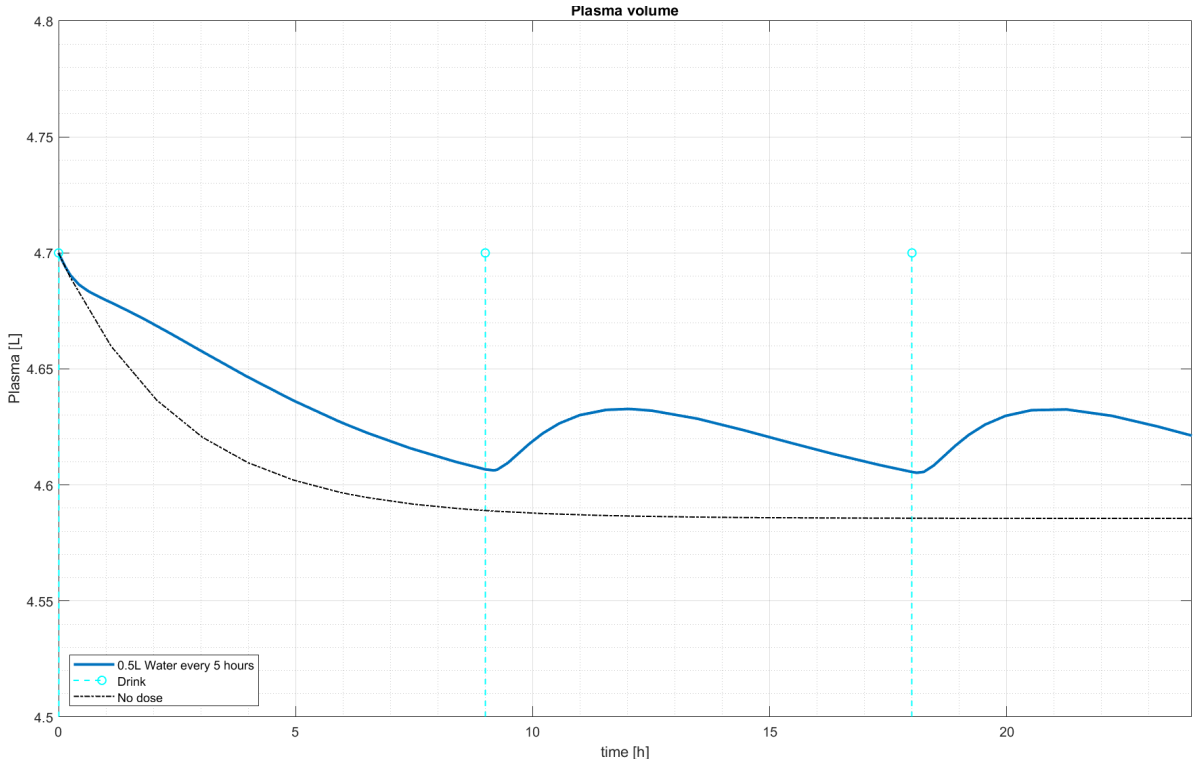

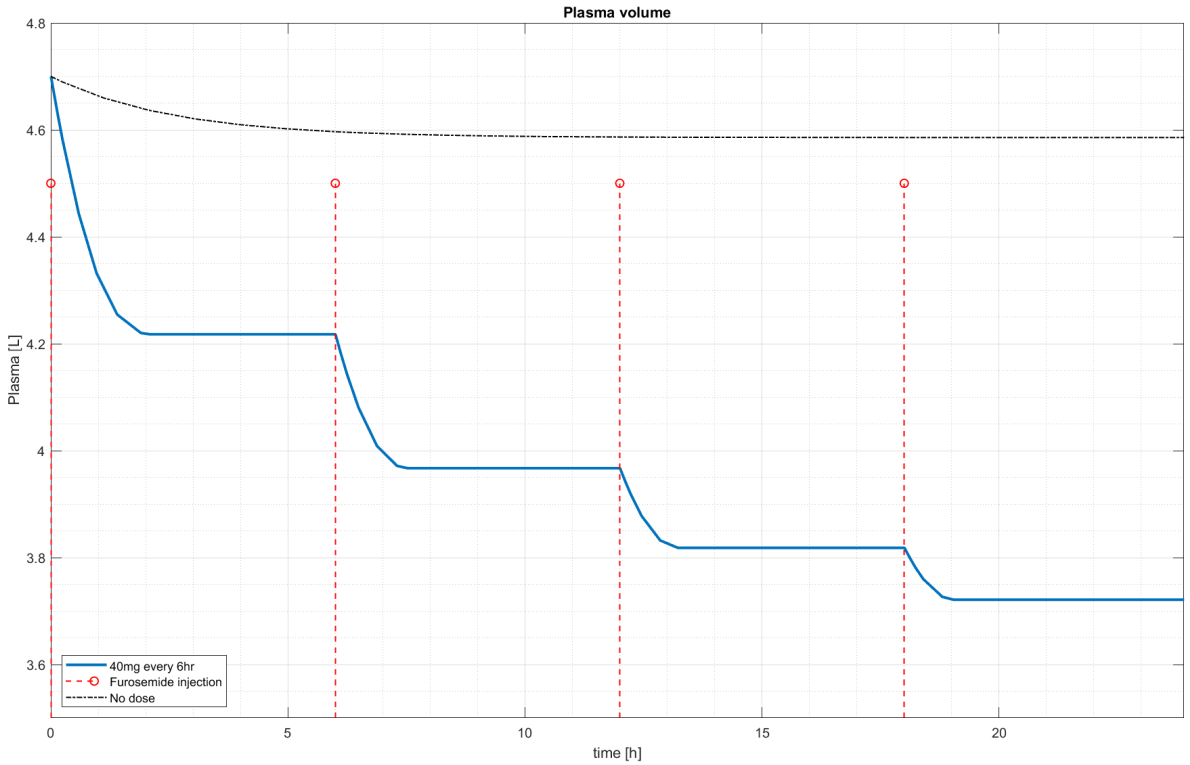

(c) Plasma output for the average patient, standard therapy (40mg furosemide every 6 hours).

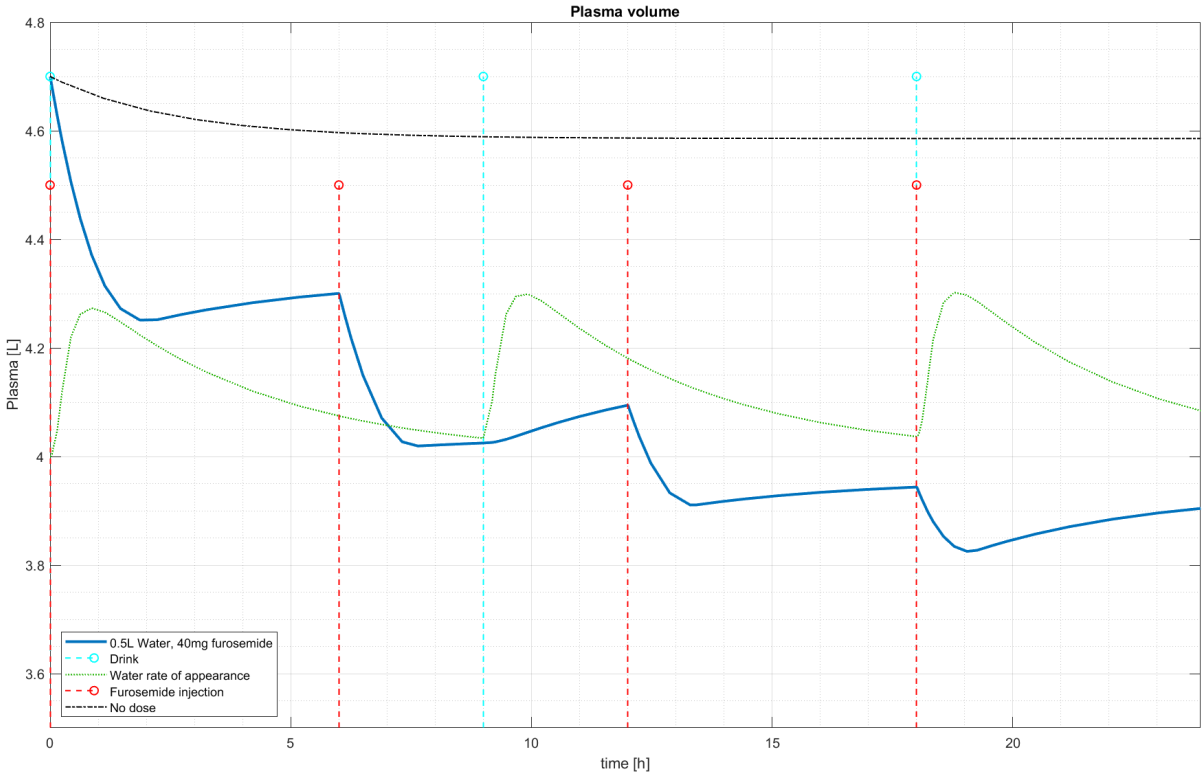

(d) Plasma output for the hydrated average patient with standard diuretic therapy.

5.4 Final Population Parameters

With the addition of the Kidney and Drinking blocks, additional parameters are introduced:

- The coefficient k_U from Equation 5.1. Since we have decided to only consider a subject in a congested state, we have decided to use the parameter associated to a state of elevated fluid volume, which in Gyenge's work has the variability (mean ± std)

$$k_U = 1.250 \pm 0.142\text{L/h}$$

- P_{NC}, the plasma volume in normal condition, for the congested patient. The distribution for this parameter is (mean ± std)

$$P_{NC} = 4.7 \pm 1.2\text{L}$$

  Which is the distribution of plasma volume at hospital admission collected by a 2014 clinical study on blood volume alterations in CHF patients treated with furosemide by the Mayo Clinic in Rochester, Minnesota[32].

- k_{SI} and k_{IP} were introduced by us when creating the drinking compartmental model. Considering that simple water absorption is quite fast we decided to set $k_{SI} = 4\text{h}^{-1}$ and $k_{IP} = 2\text{h}^{-1}$ in order to have a relatively short time constant and keeping in mind that the passage of water from stomach to intestine is faster, especially if the subject is on an empty stomach. For the purpose of creating a population dataset, we made an educated guess of a 30% inter-subject variance.

The average patient (Subject 0) is described by the parameters in Table 5.1

Table 5.1: *Simulation parameters for the average patient*

Pharmacokinetics	Cl_R	3.97	L/h	Pharmacodynamics			
	Cl_{NR}	2.02	L/h		a	0.04	L/h
	V_C	5.97	L		b	1.63	
	Cl_{d1}	1.10	L/h		c	4.45	mg/h
	V_{d1}	18.10	L		d	0.54	L/h
	Cl_{d2}	2.55	L/h				
	V_{d2}	3.01	L				
Drink	k_{SI}	4	h^{-1}	Kidney	k_U	1.25	L/h
	k_{IP}	2	h^{-1}		P_0	4.7	L
					K_{P0}	0.27	h^{-1}

The complete dataset is described in Tables 5.2 and 5.3.

Table 5.2: *PKPD population parameters*

	PK							PD			
Subject	Cl_R [L/h]	Cl_{NR} [L/h]	V_C [L]	Cl_{d1} [L/h]	V_{d1} [L]	Cl_{d2} [L/h]	V_{d2} [L]	a [mL/h]	b	c [mg/h]	d [L/h]
0	3.97	2.02	5.97	1.10	18.10	2.55	3.01	44.70	1.63	4.45	0.54
1	3.87	1.97	5.82	1.07	7.91	0.89	2.93	37.74	1.63	3.93	0.39
2	3.93	2.00	5.91	1.09	17.92	2.94	2.98	53.19	1.69	4.57	0.41
3	4.04	2.05	6.07	1.12	20.00	4.20	3.06	45.44	1.60	4.11	0.63
4	5.02	2.55	7.55	1.39	12.74	2.62	3.81	56.56	1.63	3.28	0.44
5	3.37	1.71	5.07	0.93	17.89	2.95	2.56	48.82	1.61	2.76	0.63
6	5.37	2.73	8.08	1.49	30.76	3.37	4.07	47.89	1.67	3.55	0.56
7	4.14	2.10	6.22	1.15	24.03	2.76	3.14	45.01	1.64	3.16	0.45
8	2.74	1.39	4.12	0.76	15.57	3.29	2.08	42.89	1.61	5.36	0.63
9	4.72	2.40	7.10	1.31	13.87	3.49	3.58	43.71	1.58	3.88	0.66
10	5.15	2.62	7.74	1.43	16.47	1.78	3.90	31.50	1.54	5.45	0.70
11	2.69	1.37	4.05	0.75	12.50	2.94	2.04	41.00	1.63	5.43	0.33
12	3.79	1.93	5.70	1.05	21.07	3.34	2.87	27.02	1.69	3.97	0.45
13	5.04	2.57	7.58	1.40	16.00	2.59	3.82	48.83	1.74	1.51	0.56
14	3.26	1.66	4.90	0.90	3.63	2.78	2.47	41.65	1.66	5.59	0.40
15	3.95	2.01	5.94	1.10	26.07	3.16	3.00	20.47	1.59	4.74	0.69
16	3.33	1.69	5.01	0.92	19.19	3.34	2.52	38.71	1.63	4.72	0.54
17	2.87	1.46	4.32	0.80	23.11	2.63	2.18	55.67	1.66	7.36	0.49
18	3.82	1.95	5.75	1.06	16.56	2.95	2.90	61.14	1.58	2.57	0.56
19	2.49	1.27	3.75	0.69	15.02	1.41	1.89	43.18	1.64	6.82	0.47
20	3.54	1.80	5.32	0.98	14.71	2.96	2.68	52.05	1.60	2.97	0.63

Table 5.3: *Plasma-related population parameters*

	Kidneys			Drink	
Subject	k_U	$P0$	k_{P0}	k_{SI}	k_{IP}
	[L/h]	[L]	[h^{-1}]	[h^{-1}]	[h^{-1}]
0	1.25	4.70	0.27	4.00	2.00
1	1.03	7.03	0.15	2.79	1.76
2	1.29	4.88	0.27	3.40	1.93
3	1.26	4.90	0.26	6.53	1.18
4	1.17	6.09	0.19	3.63	2.35
5	1.30	5.28	0.25	2.01	2.03
6	1.38	4.17	0.33	4.39	2.03
7	1.28	3.95	0.32	3.01	3.36
8	1.16	5.21	0.22	1.70	0.84
9	1.08	4.07	0.27	4.14	2.54
10	1.30	4.05	0.32	4.58	2.12
11	1.08	4.91	0.22	2.87	1.43
12	1.12	5.30	0.21	2.08	1.28
13	1.25	5.40	0.23	1.70	0.59
14	0.98	6.27	0.16	5.45	1.10
15	1.23	4.37	0.28	4.69	0.40
16	0.98	5.35	0.18	5.07	1.77
17	1.50	4.05	0.37	2.83	2.22
18	1.27	7.90	0.16	4.81	2.23
19	1.28	5.28	0.24	2.73	1.46
20	1.26	4.12	0.31	2.86	1.84

5.5 Linearisation

We intend to apply to the system the model predictive control strategy, which will be further explored in Chapter 6. We envision to use a strategy based on a linear model. The model we have described thus far, though, presents some non-linearities, therefore we have to linearise it before we can apply our control.

The linearisation process was done through the Model Linearizer application in Simulink®.

We consider two inputs:

- the amount of furosemide that is infused intravenously in a continuous stream, which is also the quantity that we want to control;
- the amount of water drank by the subject at a given time, which is considered as a disturbance.

The system has two outputs that are related but that will play different role in the control algorithm:

- the current plasma volume of the subject, which is the quantity that we aim to control, but cannot directly measure;
- their urine excretion rate, which is the quantity that we assume to be measurable.

The system was linearised around the working point where the expected plasma output was $y_{eq} = 3.35$L, with an expected furosemide input of $u_{eq} = 0.8$mg/h. At equilibrium the patient is not drinking constantly, therefore the disturbance is null.

The linearisation process requires the introduction of a perturbed state $\delta x = x - x_{eq}$, a perturbed input $\delta u = u - u_{eq}$, and a perturbed output $\delta y = y - y_{eq}$.
Thus the linearised system can be easily described through four matrices, A, B, C, and D.

$$\begin{cases} \delta\dot{x}(t) = A\delta x(t) + B\delta u(t) \\ \delta\dot{y}(t) = C\delta x(t) + D\delta u(t) \end{cases} \tag{5.2}$$

Our linearised system is described by the following matrices:

$$A = \begin{bmatrix} 0.3679 & 0 & 0 & 0 & 0 & 0 \\ 0.4773 & 0.6065 & 0 & 0 & 0 & 0 \\ 0 & 0 & 0.6762 & 0.0124 & 0.1565 & 0 \\ 0 & 0 & 0.0377 & 0.9852 & 0.0040 & 0 \\ 0 & 0 & 0.0789 & 6.6071 \cdot 10^{-4} & 0.8177 & 0 \\ 0.1493 & 0.3733 & -1.2484 \cdot 10^{-4} & -1.0234 \cdot 10^{-6} & -1.3342 \cdot 10^{-5} & 0.9070 \end{bmatrix} \tag{5.3}$$

$$B = \begin{bmatrix} 0 & 0.1580 \\ 0 & 0.0774 \\ 12.3872 & 0 \\ 0.3023 & 0 \\ 0.6568 & 0 \\ -0.0010 & 0.0142 \end{bmatrix} \tag{5.4}$$

$$C = \begin{bmatrix} 0 & 0 & 0 & 0 & 0 & 1 \\ 0 & 0 & 0.0153 & 0 & 0 & 9.3750 \end{bmatrix} \tag{5.5}$$

$$D = \begin{bmatrix} 0 & 0 \\ 0 & 0 \end{bmatrix} \tag{5.6}$$

To compare the non-linear system and the linearised system we introduced a sinusoidal 30% perturbation on the drug input. The results are reported in Figure 5.5.

As we can see in the figure, the two systems have very similar responses. The non-linear system is apparently less sensitive to the perturbations, probably because of the hidden action of a Saturation Block in the Kidneys subsystem which prevents the urinary output from being negative, as that would indicate a replenishment of plasma volume from the urine stored in the bladder, which is physiologically impossible.

In order to implement our control strategy, we will also need to be able to estimate the state of the system in each iteration, since in the non-linear system, the state is inaccessible.
Therefore, we need a state estimator. We chose to use a Kalman filter for this task, and we directly employed the pre-programmed Kalman Filter Block available in Simulink®.

We can tune the Kalman filter to produce an estimated state that closely matches the states we can extract from the linearised system. The results are reported in Figure 5.6. We can see how the two versions of the system's state match in steady-state.

As previously anticipated, the Kalman filter cannot access the plasma volume mea-

surements, only the urinary flow, which is however a quantity directly connected to the changes in plasma volume, and will therefore use the urinary flow measurements in order to estimate the state.

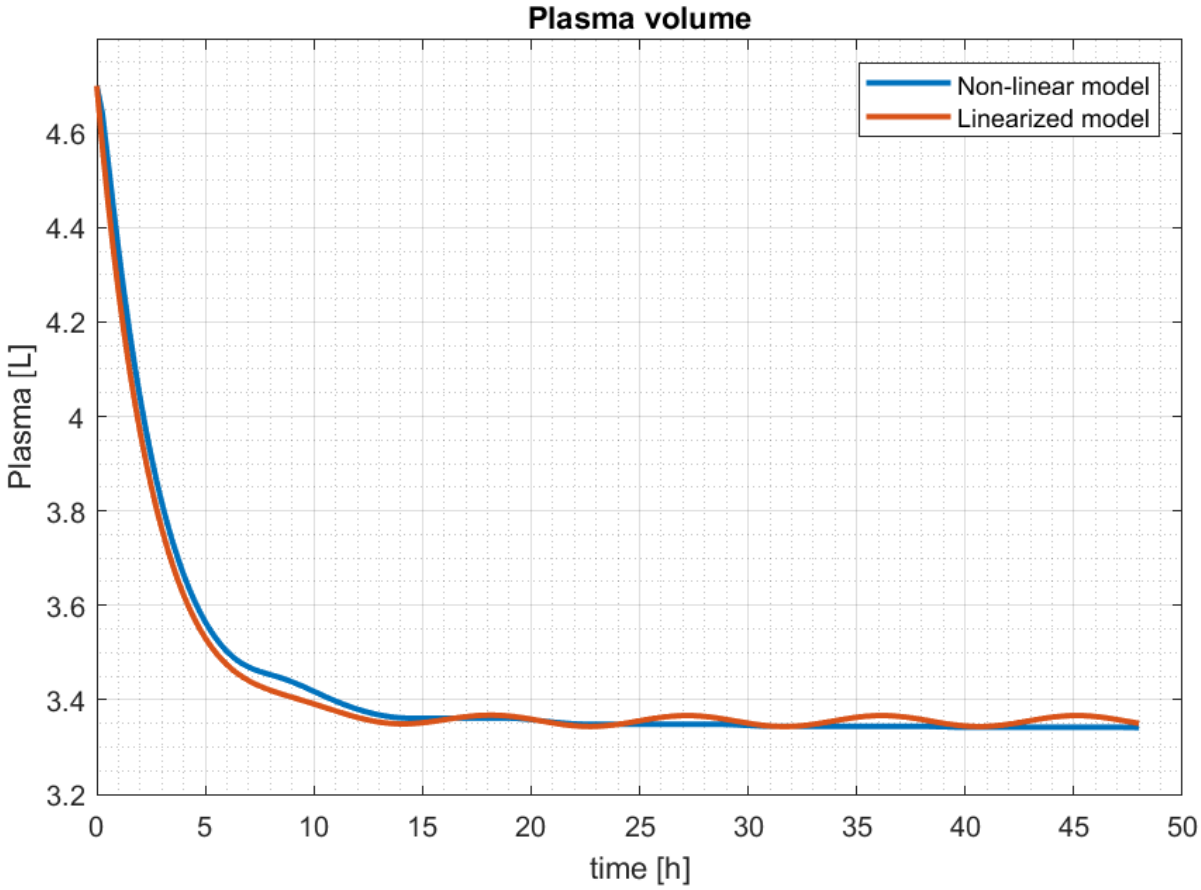

Figure 5.5: *Non-linear vs Linearised system*

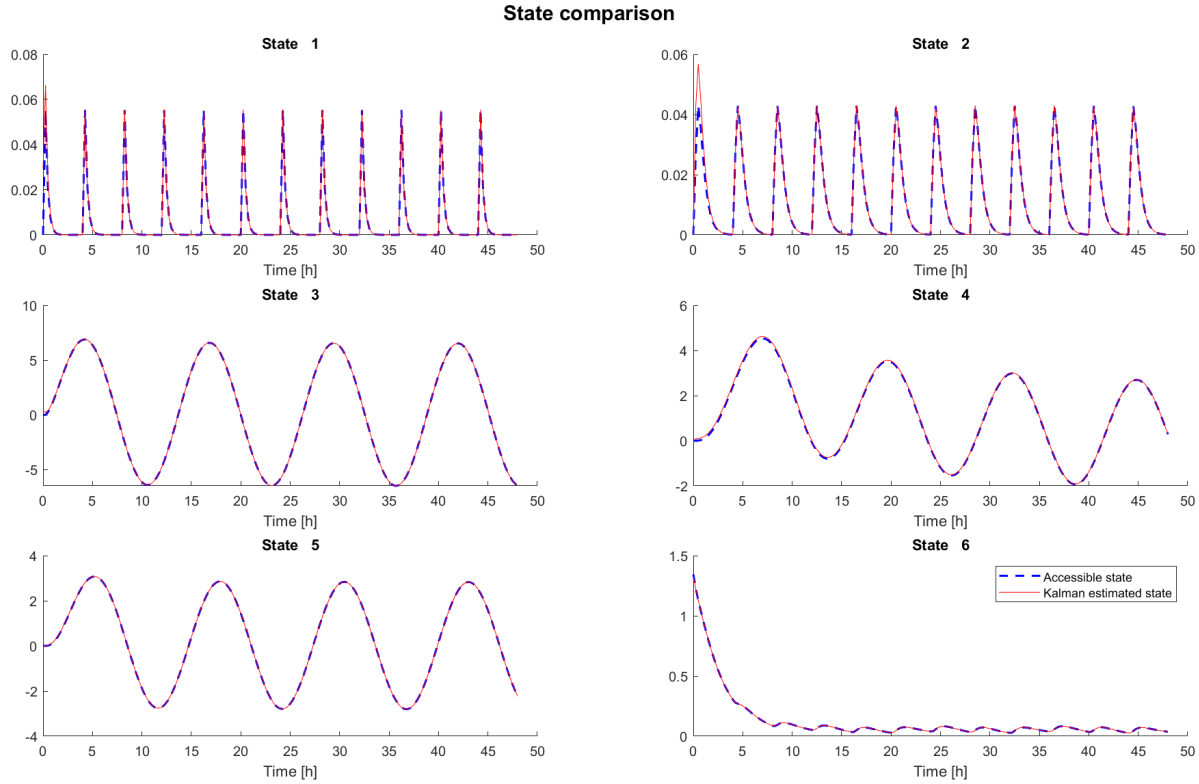

Figure 5.6: *State comparison between linearised system and Kalman filter*

Chapter 6

Control

6.1 Model Predictive Control

The term "model predictive control" (MPC) encompasses a variety of closed-loop control methods with the purpose of minimising a specific cost function.
More specifically, the key strategy of the MPC technique is the receding horizon, which consists in choosing the optimal control sequence after evaluating the predicted effect of all the possible sequences of N control actions that could be applied to system.

In other words, the MPC strategy is developed through cyclical steps:

1. Evaluate every possible sequence of N admissable control actions $\mathcal{U}(k)$, picking the sequence that yields the optimal result, as defined by the cost function.

2. Apply only the first control action out of the selected sequence and wait for the new measurement to be registered.

3. Re-evaluate all the possible sequences $\mathcal{U}(k)$ and select the optimal one.

4. Apply only the first action in the optimal sequence, wait for the next measurement from the system, and go back to step 1.

It is important to note that a solution that produces a very low cost, may not be feasible because of the system's own limitations, such as the impossibility of administering a negative dose of a drug. These limitations are described through mathematical constraints, which can be either hard or soft constraints. Hard constraints describe forbidden conditions which must never be reached by the system, while soft constraints define a set of conditions that are highly discouraged by the cost function but can still be reached by the system in order to find at least one feasible solution.

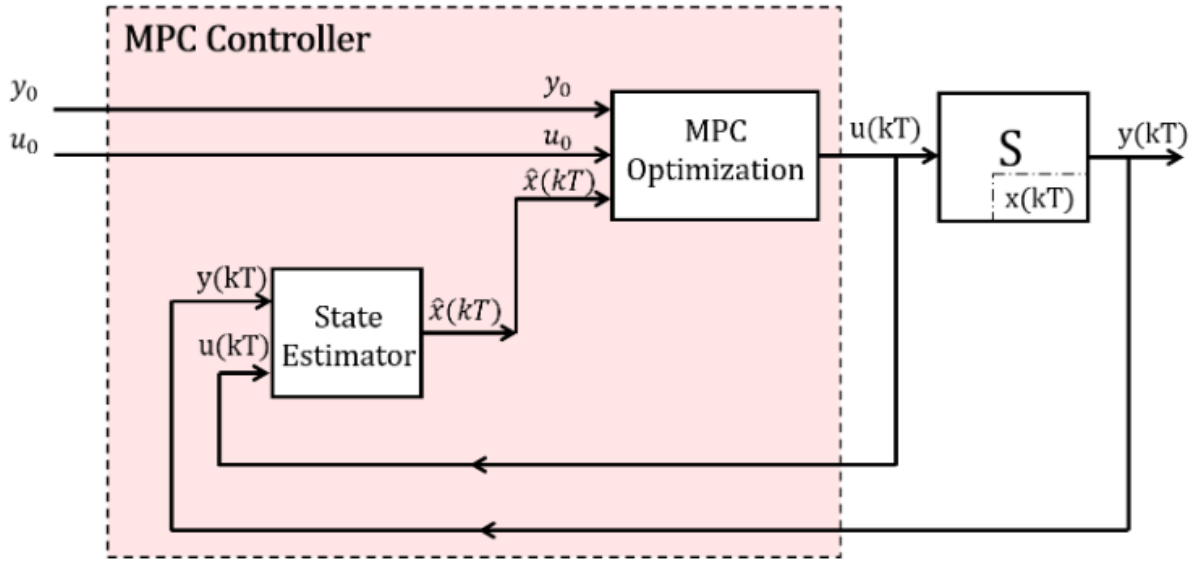

Figure 6.1: *MPC Controller Scheme*

The key elements needed to describe an MPC therefore are:

- A mathematical model of the system to be controlled,
- A cost function to optimise,
- A set of constraints

The mathematical model we will be considering is of course the linearised model that has been described thus far in Chapter 5, defined by the Equations 5.3 through 5.6.
As previously mentioned, the system has two inputs and two outputs. However, they all have different roles in our control strategy. Of the two inputs, the only one we aim to control is the amount of furosemide administered to the patient, while the other input, deriving from the patient drinking water, is considered a known, measurable disturbance. Therefore, for what concerns the controller, there system is single input.

Likewise, while the model includes two outputs, the plasma volume and the urinary flow, only the latter is measurable and therefore accessible to the state estimator and the controller. Hence, the MPC will only consider one output, even though the plant will produce two.

Thus, for the purpose of control, this system is single input, single output (SISO).

The cost function (Equation 6.1) is a quadratic cost function for reference tracking, which means that we want the MPC to track a reference signal in output y_0, but without

straying too much from a reasonable, pre-determined, input u_0.

$$J = \sum_{i=0}^{N-1} [(\hat{y}(k+i) - y_0(k+i))^T Q(\hat{y}(k+i) - y_0(k+i)) + (u(k+i) - u_0(k+i))^T R(u(k+i) - u_0(k+i))] \tag{6.1}$$

where $\hat{y}(k+i)$ is the predicted output at time $k+i$ in response to the previous control action $u(k+i-1)$, and $u(k+i)$ is the control action delivered at time $k+i$.

Q and R are the parameters that regulate how aggressive the control will be. Since we are dealing with a SISO system, Q, $R \in \mathbb{R}^1$, and we can rewrite Equation 6.1 as

$$J = \sum_{i=0}^{N-1} \left[\frac{Q}{R} (\hat{y}(k+i) - y_0(k+i))^2 + (u(k+i) - u_0(k+i))^2 \right] \tag{6.2}$$

This underlines how the parameter Q/R regulates the controller's aggressiveness. If Q is higher than R, the controller will have a more aggressive approach because it will be less penalised for the control actions that deviate farther from u_0, while it will cost more to deviate from the target output y_0. On the other hand, if R is higher than Q, the MPC algorithm will favour solutions that do not impose control actions much different from the reference.

Lastly, we had to set a hard constraint on the input so that the amount of drug injected could not be negative, since once the drug is delivered, it cannot be taken out of the body. So, our constraint is

$$u \geq 0 \tag{6.3}$$

And in the linearised system, it becomes

$$\delta u \geq u_{eq} \tag{6.4}$$

It is important to note that implementing the strategy as it has been described until now will not allow us to perfectly match the output we are tracking. This is because while the MPC tries to match the reference output profile as close as possible, the cost function penalises the control actions that are furthest from the reference input profile. The MPC has to reach a compromise and that results in an output that will always present an offset from the actual reference.

The offset can be removed by adding an integral action to the controller, but we will not implement this technique because of limited time.

6.2 Results

6.2.1 Average Subject

By applying an MPC controller to the system we wanted to obtain a better performance than what the standard diuretic therapy could achieve (Figure 6.2).

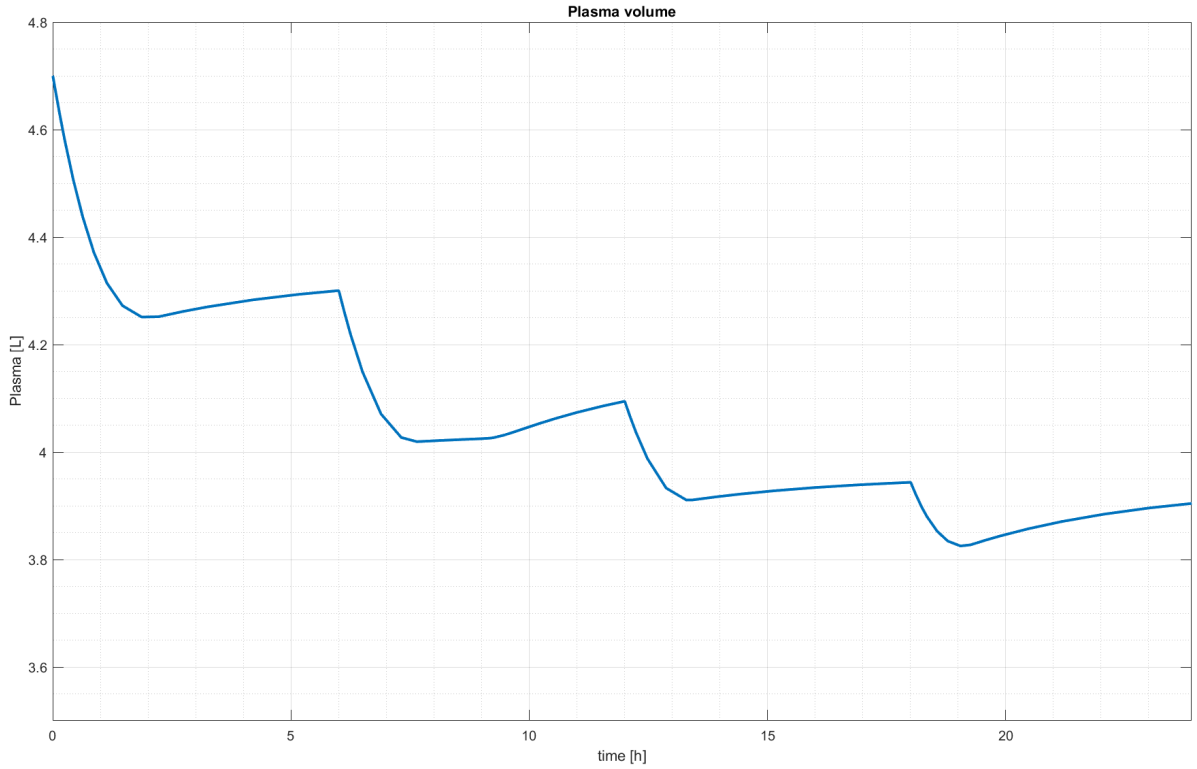

Figure 6.2: *Plasma output for the hydrated average patient with standard diuretic therapy (40mg furosemide every 6 hours).*

Figure 6.3 shows clear improvements in performance with the employment of an MPC controller with respect to the standard case. The two figures are also meant to show how different tunings of the controller, through the cost parameters Q and R, can change the output.

In Figure 6.3a, we set $Q = 0.1$ and $R = 1$, therefore any deviance from the input reference is penalised by the cost function more than any deviance from the tracking reference. As a consequence, the controller doesn't have a very aggressive approach, and there are smaller peaks in the control profile. In Figure 6.3b, on the other hand, the MPC was set to a more aggressive behaviour ($Q = 1$, $R = 0.1$), thus penalising more the distance from the tracking reference, which results in higher control actions that allow the system to maintain a smaller offset in output.

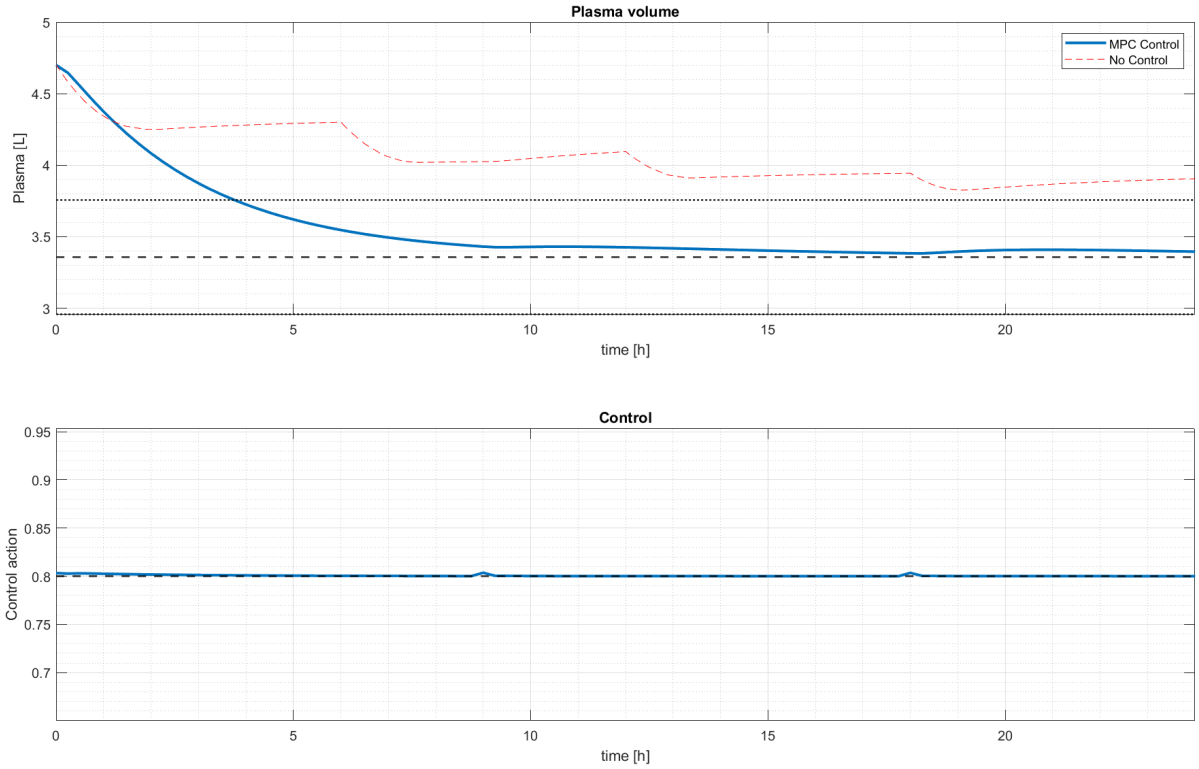

(a) MPC output and control actions executed. The MPC is tuned to be less aggressive.

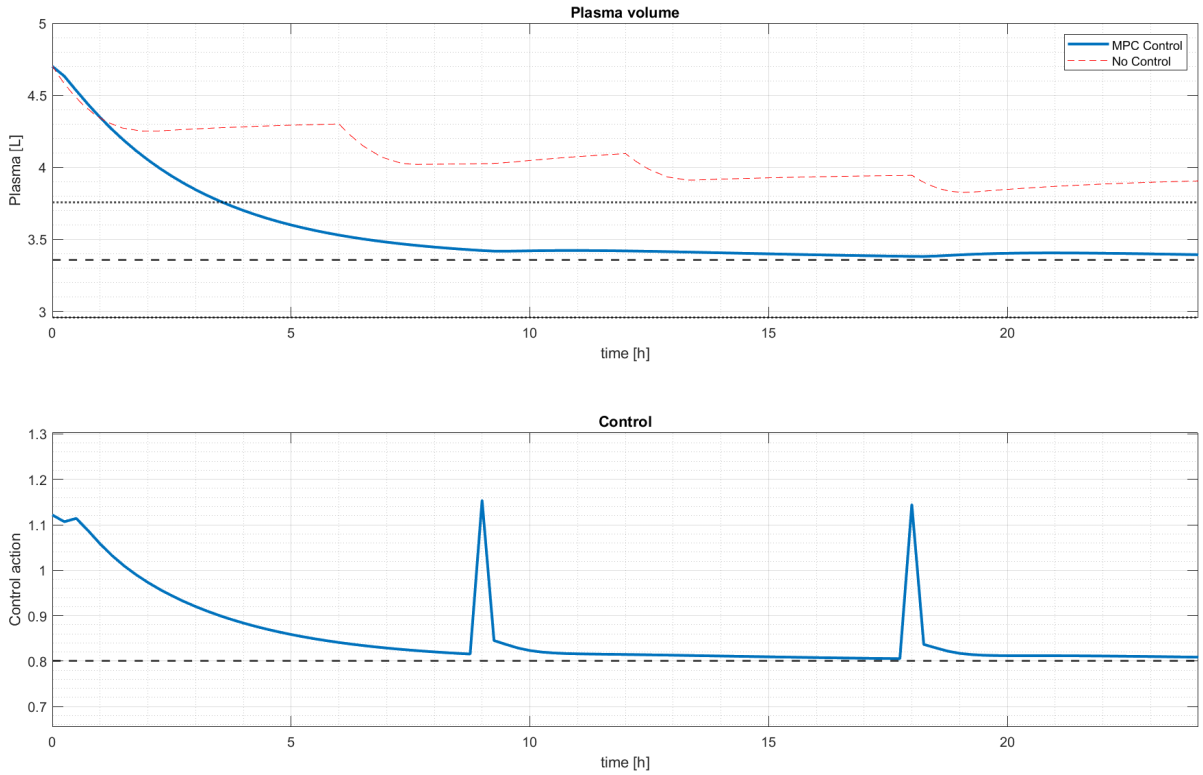

(b) MPC output and control actions executed. The MPC is tuned to be more aggressive.

Figure 6.3: *Results of the control actions with different tunings for the average patient.*

6.2.2 Population Simulation

Finally, we run the simulation on the entire population. The results are shown in Figure 6.4.

It is even more clear that the current version of the MPC, without an integral action, is unable to reach the target plasma volume. The greater the distance between the original conditions used for the linearisation, the greater is the offset. Still, most of the subjects reach a steady-state plasma volume within the 2.5-3.9L range that was the expected plasma volume at discharge for the patients in the Mayo Clinic study[32], where the actual range of plasma volume at discharge was 3.0-5.9L.

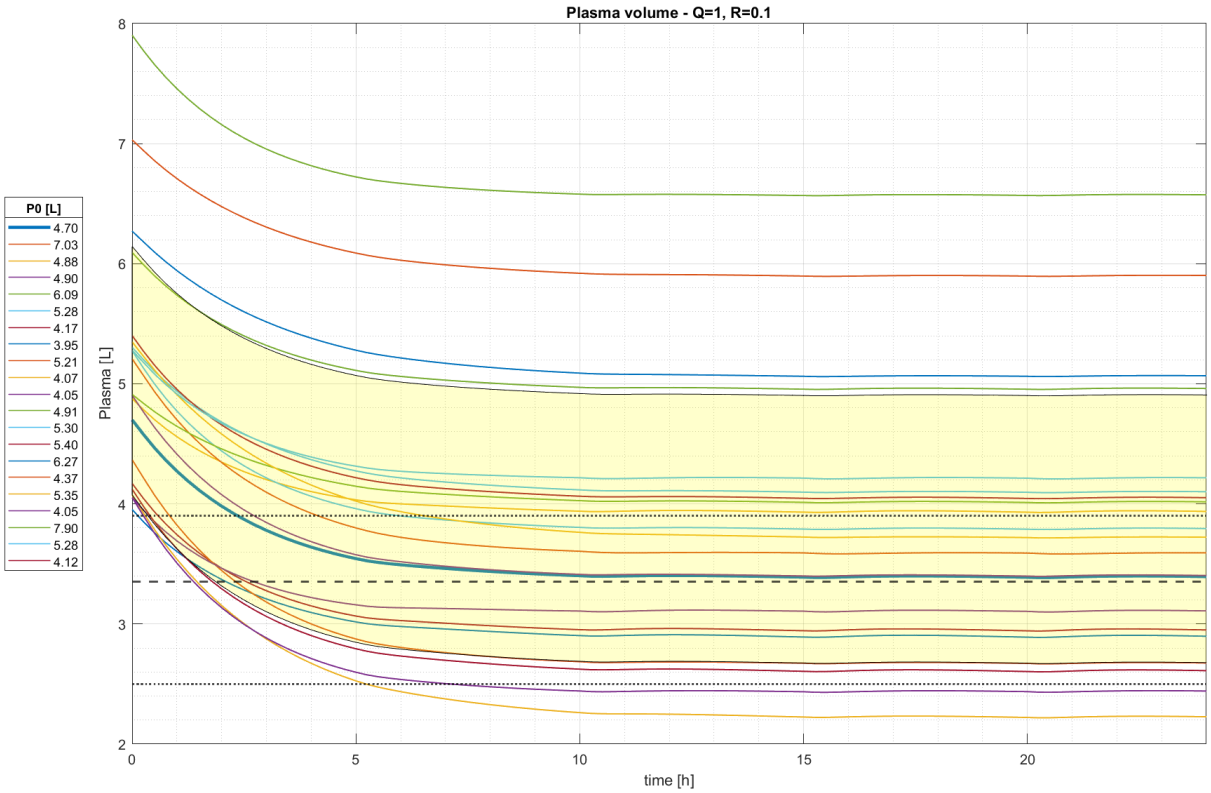

Figure 6.4: *Simulated population - MPC results. The yellow area denotes ±1 std confidence interval. In bold, the average patient.*

Chapter 7

Conclusion

When we started this project, we knew that it was a promising and ambitious project and that we would not be able to address all the aspects of diuretic therapy against congestion in patients with heart failure.

Indeed, we encountered several challenges.

First and foremost, a lack of contemporary literature on furosemide and its PKPD description through a reliable mathematical model. Most of the pharmacology research on the drug was made in the 1970s and 1980s, with results that often were not comparable from study to study, especially for what concerns the estimation of the parameters needed for a working mathematical model. It is safe to assume that new insights on furosemide would be possible if PKPD models were to be reassessed using the pharmaceutical techniques available today, but there is currently a lack of a drive to further explore such a clinically established drug.

Moreover, the renal system is one of the most complex biological systems in the human body. So much so, that some of its workings are still being studied nowadays. This, of course, means that reliable and complete mathematical models of the kidneys and the renal system are elusive, especially if one is not directly interested in the more mechanical descriptions of the fluidodynamics involved in renal activity. Because of this, as discussed in Chapter 4, we only managed to find two models that could be adapted to our purposes.

Another critical point was the modelling of the transportation of liquids within the human organism. This concept was simplified in this work, but the total fluid volume within a human body is comprised of two major compartments: the intracellular fluid volume and the extracellular fluid volume. Plasma can be considered a portion of the latter.

There are constantly exchanges between these compartments, which are physiologically controlled by several different mechanisms, and the estimation of the three volumes

is not straightforward and therefore translating this concepts into workable mathematical models is challenging.
In this work, we chose to consider the plasma compartment on its own, with the understanding that reality is much more complex and, ideally, the existence of the extracellular fluid compartment should not be discarded.

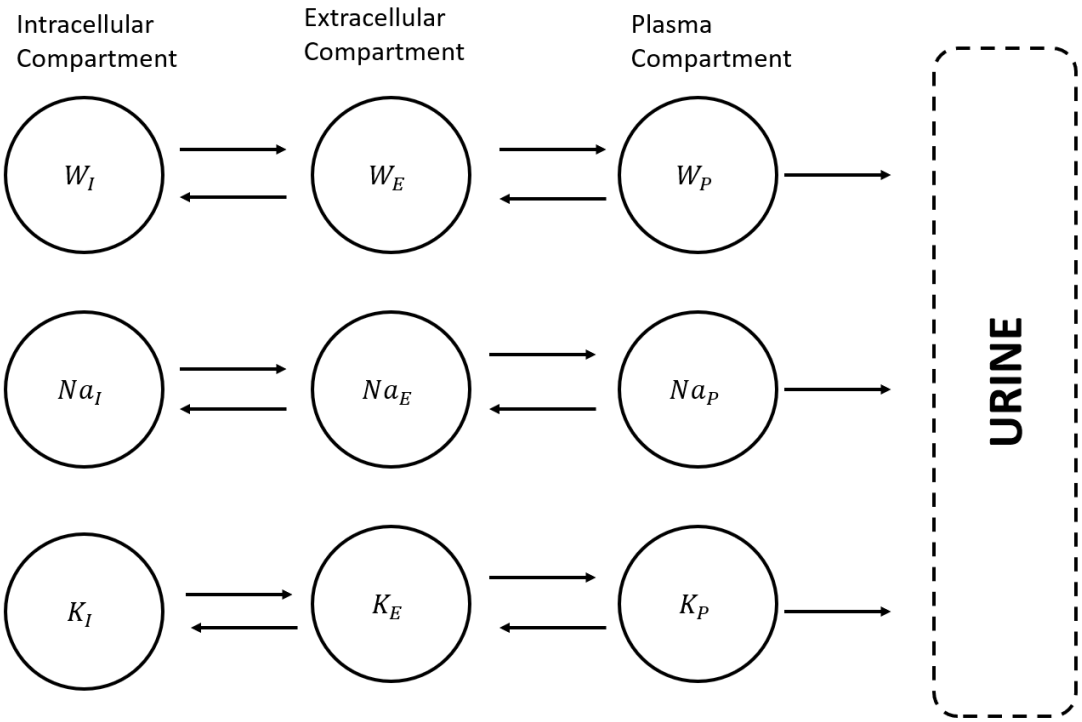

Figure 7.1: *Schematic representation of the exchanges between fluid compartments in the body. Not represented, the intercorrelations between the ion concentrations and the rates of exchange between compartments.*

Additionally, this project was concerned with dealing with congestive heart failure, which is a complex and multifaced health condition that complicates matters extensively. Most of the literature that has been consulted for this work, about both the renal system and furosemide, focuses on *healty* subjects, which have remarkably different responses than CHF patients, as was confirmed by our clinical partners.

Heart failure deeply imbalances the activity of the cardiac and renal systems, and using a model which is validated only against data collected from healthy individuals is a non-negligible bias, although it was a necessary starting point.

In spite of all these challenges and issues, which, understandably, could not be all fully addressed within the scope and the limited time frame of this work, we still successfully managed to set up a model that integrated both renal activity and its response to diuretic treatment in the form of furosemide delivery. In addition to that we successfully introduced a control algorithm that managed to produce a better outcome in terms of

decongestion than what the most common clinical therapy provides.

Although this work is just the opening act of the research on automatic control of diuretic therapy against congestion in heart failure patients, we have shown that it is a feasible endeavour and we have set up the groundwork on which we can keep building to achieve more and more accurate results.

Appendices

Appendix A

Uttamsingh's Model, Extended

As seen in Chapter 4, several of the functions that make up the Kidney and Hormonal subsystems are piecewise functions. Here are reported the extended equations that define those quantities.

A.1 Kidney System

Glomerular filtration rate (GFR), dependent on the arterial pressure P_A:

$$GFR = \begin{cases} 0.0 & \text{if } P_A \leq 20.0 \text{ mmHg} \\ 1.29P_A - 38.4 & \text{if } 20.0 < P_A \leq 75.0 \text{ mmHg} \\ -8.08 \cdot 10^{-3} P_A^2 + 2.195P_A - 13.6 & \text{if } 75.0 < P_A \leq 120.0 \text{ mmHg} \\ 0.035P_A + 129.2 & \text{if } P_A > 120 \text{ mmHg} \end{cases} \tag{A.1}$$

Fraction of water load reabsorbed in the distal tubule, dependent on the concentration of antidiuretic hormone ADH ($B_{W,DT} = f(ADH)$):

$$B_{W,DT} = f(ADH) = \begin{cases} 0.0 & \text{if } ADH \leq 0.765 \text{ munits} \cdot \text{L}^{-1} \\ 0.383ADH - 0.293 & \text{if } 0.765 < ADH \leq 3.0 \text{ munits} \cdot \text{L}^{-1} \\ -38.3 \cdot 10^{-3} ADH^2 + 0.364ADH + 0.109 & \text{if } 3.0 < ADH \leq 15.0 \text{ munits} \cdot \text{L}^{-1} \\ 1.2 \cdot 10^{-3} ADH + 0.9653 & \text{if } ADH > 5.0 \text{ munits} \cdot \text{L}^{-1} \end{cases} \tag{A.2}$$

Fraction of reabsorbed sodium in the distal tubule over the rate of flow of sodium into the distal tubule, dependent on the concentration of aldosterone ALD ($\frac{R_{Na,DT}}{J_{Na,DT}} = f(ALD)$):

$$\frac{R_{Na,DT}}{J_{Na,DT}} = f(ALD) = \begin{cases} 0.6 & \text{if } ALD \leq 0 \text{ ng} \cdot \text{L}^{-1} \\ 0.003ALD - 0.596 & \text{if } 0 < ALD \leq 85.0 \text{ ng} \cdot \text{L}^{-1} \\ 0.21 \cdot 10^{-3}ALD + 0.833 & \text{if } 85.0 < ALD \leq 800.0 \text{ ng} \cdot \text{L}^{-1} \\ 1 & \text{if } ALD > 800.0 \text{ ng} \cdot \text{L}^{-1} \end{cases} \tag{A.3}$$

Potassium excretion rate due to aldosterone ($U_{K,ALD} = f_K(ALD)$)

$$U_{K,ALD} = f_K(ALD) = \begin{cases} 0.28 \cdot 10^{-3}ALD + 6.2 \cdot 10^{-3} & \text{if } ALD \leq 85.0 \text{ ng} \cdot \text{L}^{-1} \\ 0.09 \cdot 10^{-3}ALD + 22.4 \cdot 10^{-3} & \text{if } ALD > 85.0 \text{ ng} \cdot \text{L}^{-1} \end{cases} \tag{A.4}$$

A.2 Hormonal System

The control of ADH concentration is the section of this model that is most difficult to represent in a graph, because the release rate for ADH, $ADHS$ is a piecewise function that depends on two variables that are they themselves the outputs of two separate piecewise functions of different variables.

$$ADHS = \begin{cases} (17\Delta V_{EX} \cdot ADHSV + ADHSP)(17\Delta V_{EX} + 1)^{-1} & \text{if } P_{OS} > 299.6 \text{ mOsm} \cdot \text{L}^{-1} \\ & \text{and } \Delta V_{EX} > 2.01 \text{ L} \\ ((33\Delta V_{EX} - 32)ADHSV + ADHSP)(33\Delta V_{EX} - 31)^{-1} & \text{if } P_{OS} > 299.6 \text{ mOsm} \cdot \text{L}^{-1} \\ & \text{and } 1 < \Delta V_{EX} \leq 2 \text{ L} \\ \frac{1}{2}(ADHSV + ADHSP) & \text{for all other conditions} \end{cases} \tag{A.5}$$

where P_{OS} is the plasma osmolarity; and $ADHSV$ and $ADHSP$ are respectively the release rate for ADH due to deviations of the extracellular fluid $\Delta V_{EX} = V_{EX} - V_{EX,NC}$ from the normal volume $V_{EX,NC}$, and the release rate of ADH due to the changes in plasma osmolarity, modelled as a dependency on the concentration of sodium in plasma Na_P.

$$ADHSV = \begin{cases} 0.0 & \text{if } \Delta V_{EX} \geq 1.8 \text{ L} \\ 0.15 - 0.083\Delta V_{EX} & \text{if } 1.8 > \Delta V_{EX} \geq 1.0 \text{ L} \\ 0.813 - 0.75\Delta V_{EX} & \text{if } 1 > \Delta V_{EX} \geq -1.2 \text{ L} \\ 1.71 & \text{if } \Delta - 1.2 > V_{EX} \text{ L} \end{cases} \tag{A.6}$$

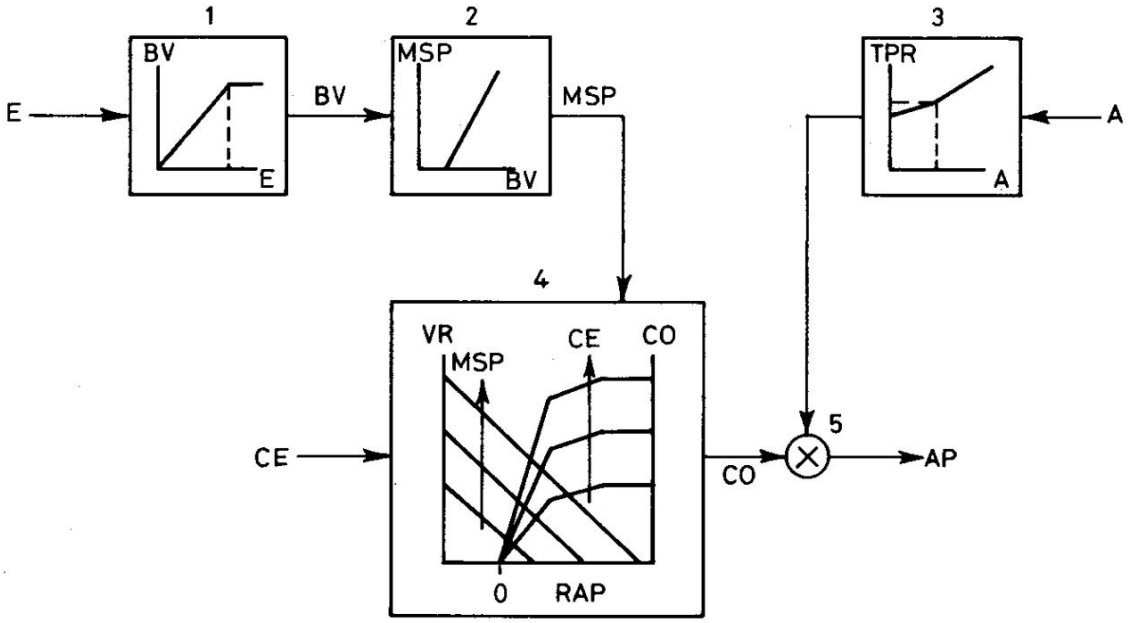

Figure A.1: *Block diagram of the cardiovascular subsystem from[26]. Blocks: 1 - blood volume, 2 - mean systemic pressure, 3 - total peripheral resistance, 4 - cardiac output, 5 - arterial pressure.*

$$ADHSP = \begin{cases} 0.73Na_P - 103.34 & \text{if } Na_P \geq 141.9 \text{ mOsm} \cdot \text{L}^{-1} \\ 0.06Na_P - 8.04 & \text{if } Na_P < 141.9 \text{ mOsm} \cdot \text{L}^{-1} \end{cases} \tag{A.7}$$

The other function dependent on the level of ADH present in plasma is the rate of ADH clearance Cl_{ADH}, which is approximated by the function

$$Cl_{ADH} = \begin{cases} 0.206 & \text{if } ADH > 4.0 \text{ munits} \cdot \text{L}^{-1} \\ 0.374 - 0.042ADH & \text{if } ADH \leq 4.0 \text{ munits} \cdot \text{L}^{-1} \end{cases} \tag{A.8}$$

Finally, the aldosterone activation due to the level of angiotensin II (A) seen in Eq. 4.24 is approximated by

$$f(ANGII) = \begin{cases} A & \text{if } A < 18.0 \text{ ng} \cdot \text{L}^{-1} \\ 4.43A - 61.7 & \text{if } 18.0 \leq A < 34.0 \text{ ng} \cdot \text{L}^{-1} \\ 0.78A + 62.5 & \text{if } A \geq 34.0 \text{ ng} \cdot \text{L}^{-1} \end{cases} \tag{A.9}$$

A.3 Cardiovascular System

The cardiovascular subsystem modelled by Uttamsingh is quite more complex than what we have considered in Chapter 4.1.3.

A.3.1 Block 1: Blood Volume

The blood volume (Block 1 in Figure A.1) represents an empirical relationship between V_B and the extracellular fluid volume V_{EX} such that

$$V_B = \begin{cases} 0.33V_{EX} & \text{if } V_{EX} < 21 \text{ L} \\ 0.015V_{EX} & \text{if } v_{EX} \geq 21 \text{ L} \end{cases} \tag{A.10}$$

A.3.2 Block 2: Mean Systemic Pressure

The mean systemic pressure P_{MS} is dependent on blood volume and described as

$$P_{MS} = 3.5(V_B - 3) \tag{A.11}$$

A.3.3 Block 3: Total Peripheral Resistance

The total peripheral resistance TPR to the blood flow of Block 3 was not considered by Cloutman and is dependent on the level of angiotensin II in plasma.

$$TPR = \begin{cases} 19 + 0.037A & \text{if } A \leq 27 \text{ ng} \cdot \text{L}^{-1} \\ 12.2 + 5.44 \log A_{10} & \text{if } A > 27 \text{ ng} \cdot \text{L}^{-1} \end{cases} \tag{A.12}$$

A.3.4 Block 4: Cardiac Output

The cardiac output (Block 4) is the most complex section of the system. It depends on two curves, one relating the venous return VR to the right atrial pressure P_{RA} and P_{MS}, the other relating the cardiac output CO to both P_{RA} and a generalised index of cardiac effectiveness CE:

$$VR = f(P_{RA}, P_{MS}) \tag{A.13}$$

$$CO = g(P_{RA}, CE) \tag{A.14}$$

In particular, Uttamsingh identifies a specific curve for each of these families. For Eq. A.13:

$$VR = \frac{P_{MS} - P_{RA}}{R_{VR}} \tag{A.15}$$

where $R_{VR} = \alpha$ is the return venous resistance, with α a constant parameter.

For Eq. A.14, the selected function g has significant non linearities and it is approximated by four piecewise linear equations of the form

$$CO = a_i P_{RA} + b_i \tag{A.16}$$

where a_i and b_i change based on the operating ranges of both P_{RA} and CE. The possible pairs (a_i,b_i) associated with each combination of ranges are provided in Table A.1.

CE is equally complex to approximate, as it is dependent on both sodium and potassium concentrations in plasma:

$$CE = \frac{1}{2}(CE_{Na} + CE_K) \tag{A.17}$$

$$CE_K = \begin{cases} 1.0 & \text{if } K_P < 6.5 \text{ mOsm} \cdot \text{L}^{-1} \\ -0.065K_P + 1.43 & \text{if } K_P \geq 6.5 \text{ mOsm} \cdot \text{L}^{-1} \end{cases} \tag{A.18}$$

$$CE_{Na} = \begin{cases} 1.0 & \text{if } Na_P < 148.0 \text{ mOsm} \cdot \text{L}^{-1} \\ -0.0125Na_P + 2.85 & \text{if } Na_P \geq 148.0 \text{ mOsm} \cdot \text{L}^{-1} \end{cases} \tag{A.19}$$

Heart performance balances venous return and cardiac output, according to the Frank-Starling law. So, the operating right atrial pressure $P_{RA,eq}$ is given by solving

$$f(P_{RA,eq}, P_{MS}) = g(P_{RA,eq}, CE) \tag{A.20}$$

which, if using the equations above, solves to

$$P_{RA,eq} = \frac{P_{MS} - b_i R_{VR}}{1 + a_i R_{VR}} \tag{A.21}$$

Once computed, $P_{RA,eq}$ can be used to calculate CO from Equation A.16.

A.3.5 Block 5: Arterial Pressure

Finally, the arterial pressure, which depends on the cardiac output and the total peripheral re is such that

$$P_A = CO \cdot TPR \tag{A.22}$$

Table A.1: *Parameters (a_i,b_i) as functions of the operating ranges of P_{RA} and CE.*

	$P_{RA} \leq 0$		$0 < P_{RA} \leq 2$		$2 < P_{RA} \leq 4$		$P_{RA} > 4$	
CE	a_1	b_1	a_2	b_2	a_3	b_3	a_4	b_4
$CE > 0.85$	0	0	3.0	5.250	0.875	9.50	0	13.00
$0.85 \geq CE > 0.62$	0	0	2.50	3.75	0.625	7.50	0	8.75
$0.62 > CE$	0	0	1.7	2.125	0.375	4.75	0	6.25

References

[1] Britsh Heart Foundation. *Heart failure: a blueprint for change*. 2020. URL: https://www.bhf.org.uk/-/media/files/health-intelligence/heart-failure-a-blueprint-for-change.pdf (visited on 2023-04-13).

[2] Pellicori, P., Kuldeep, K., and Clark, A. L. "Fluid Management in Patients with Chronic Heart Failure". In: *Card Fail Rev.* 1.2 (2015), pp. 90–95. DOI: https://doi.org/10.15420%2Fcfr.2015.1.2.90.

[3] Mullens, W., Damman, K., Harjola, V. P., et al. "The use of diuretics in heart failure with congestion — a position statement from the Heart Failure Association of the European Society of Cardiology". In: *Eur J Heart Fail.* 21.2 (2019), pp. 137–155. DOI: https://doi.org/10.1002/ejhf.1369.

[4] Krämer, B. K., Schweda, F., and Riegger, G. A. J. "Diuretic treatment and diuretic resistance in heart failure". In: *Am J Med.* 106.1 (1999), pp. 90–96. DOI: https://doi.org/10.1016/s0002-9343(98)00365-9.

[5] Toffanin, C. et al. "Artificial pancreas: MPC design from clinical experience". In: *J. Diabetes Sci. Technol.* 7.6 (2013), pp. 1470–1483. DOI: https://doi.org/10.1177/193229681300700607.

[6] Kropff, J., Favero, S. D., Place, J., et al. "2 month evening and night closed-loop glucose control in patients with type 1 diabetes under free-living conditions: a randomised crossover trial". In: *Lancet Diabetes Endocrinol.* 3.12 (2015), pp. 939–947. DOI: https://doi.org/10.1016/S2213-8587(15)00335-6.

[7] Encyclopaedia Britannica. *Osmoregulation*. URL: https://www.britannica.com/science/osmoregulation (visited on 2023-01-08).

[8] National Institute of Diabetes and Digestive and Kideny Diseases. *Your Kidneys and How They Work*. URL: https://www.niddk.nih.gov/health-information/kidney-disease/kidneys-how-they-work (visited on 2023-01-08).

[9] Lote, C. J. *Principles of Renal Physiology, 5th edition*. Springer, 2012. ISBN: 9781461437840.

[10] URL: https://www.topperlearning.com/answer/describe-the-structure-of-a-nephron-with-the-help-of-a-labelled-diagram/wvudt1bb (visited on 2023-01-08).

[11] Encyclopaedia Britannica. *Vasopressin*. URL: https://www.britannica.com/science/vasopressin (visited on 2023-04-04).

[12] Cuzzo, B., Padala, S. A., and Lappin., S. L. *Physiology, Vasopressin*. StatPearls [Internet]. URL: https://www.ncbi.nlm.nih.gov/books/NBK526069/ (visited on 2023-04-04).

[13] URL: https://www.docsity.com/en/adh-diagram-homeostasis-biology-lecture-slides/242980/ (visited on 2023-01-08).

[14] Kidney Digest. *RAAS and ADH*. URL: https://www.kidneydigest.com/ras-anti-diuretic-hormone/ (visited on 2023-01-08).

[15] Chen, J. S., Sabir, S., and Al Khalili, Y. *Physiology, Osmoregulation and Excretion*. StatPearls [Internet]. URL: https://www.ncbi.nlm.nih.gov/books/NBK541108/ (visited on 2023-01-08).

[16] Encyclopaedia Britannica. *Aldosterone*. URL: https://www.britannica.com/science/aldosterone (visited on 2023-04-04).

[17] Fountain, J. H. and Lappin, S. L. *Physiology, Renin Angiotensin System*. StatPearls [Internet]. URL: https://www.ncbi.nlm.nih.gov/books/NBK470410/ (visited on 2023-01-08).

[18] URL: https://en.wikipedia.org/wiki/Renin%E2%80%93angiotensin_system#/media/File:Renin-angiotensin-aldosterone_system.svg (visited on 2023-01-08).

[19] Ellison, D. H. "Clinical Pharmacology in Diuretic Use". In: *Clinical Journal of the American Society of Nephrology* 14.8 (2019), pp. 1248–1257. DOI: 10.2215/CJN.09630818.

[20] Drugs.com. *Loop diuretics*. URL: https://www.drugs.com/drug-class/loop-diuretics.html (visited on 2022-11-23).

[21] Cox, Z. L. and Testani, J. M. "Loop diuretic resistance complicating acute heart failure". In: *Heart Fail Rev* 25 (2020), pp. 133–145. DOI: https://doi.org/10.1007/s10741-019-09851-9.

[22] Grogan, S. and Preuss, C. V. *Pharmacokinetics*. StatPearls [Internet]. URL: https://www.ncbi.nlm.nih.gov/books/NBK557744/ (visited on 2023-04-04).

[23] Van Wart, S. A. et al. "Population-based meta-analysis of furosemide pharmacokinetics". In: *Biopharmaceutics and Drug Disposition* 35.2 (2014), pp. 119–133. DOI: https://doi.org/10.1002/bdd.1874.

[24] Farinde, A. *Overwiew of Pharmacodynamics*. Ed. by Manuals, M. URL: https://www.merckmanuals.com/professional/clinical-pharmacology/pharmacodynamics/overview-of-pharmacodynamics (visited on 2023-04-04).

[25] Ponto, L. L. and Schoenwald, R. D. "Furosemide (frusemide). A pharmacokinetic/ pharmacodynamic review (Part II)". In: *Clin Pharmacokinet.* 18.6 (1990), pp. 460–471. DOI: https://doi.org/10.2165/00003088-199018060-00003.

[26] Uttamsingh, R., Leaning, M., Bushman, J., et al. "Mathematical model of the human renal system". In: *Med. Biol. Eng. Comput.* 23 (1985), pp. 525–535. DOI: https://doi.org/10.1007/BF02455306.

[27] Cloutman, R. "Mathematical Modelling of Renal Functions within a Simulated Clinical Environment". In: *Transactions on Biomedicine and Health* 4 (1997). DOI: https://doi.org/10.2495/BIO970081.

[28] Kiil, F. and Ostensen, J. "Essentials of glomerulotubular balance". In: *Acta Physiol Pharmacol Bulg.* 15.1 (1989). PMID: 2672697, pp. 3–12.

[29] Pathway Medicine. *Glomerulortubular Balance.* URL: https://www.pathwaymedicine.org/glomerulotubular-balance (visited on 2023-03-20).

[30] Gyenge, C. C. et al. "Mathematical model of renal elimination of fluid and small ions during hyper- and hypovolemic conditions". In: *Acta Anaesthesiologica Scandinavica* 47.3 (2003), pp. 122–137. DOI: https://doi.org/10.1034/j.1399-6576.2003.00037.x.

[31] Gyenge, C. C. et al. "Transport of fluid and solutes in the body I. Formulation of a mathematical model". In: *American journal of physiology. Heart and circulatory physiology* 277.3 (1999), H1215–H1227. DOI: https://doi.org/10.1152/ajpheart.1999.277.3.H1215.

[32] Miller, W. L. and Mullan, B. P. "Understanding the Heterogeneity in Volume Overload and Fluid Distribution in Decompensated Heart Failure Is Key to Optimal Volume Management". In: *JACC: Heart Failure* 2.3 (2014), pp. 298–305. DOI: https://doi.org/10.1016/j.jchf.2014.02.007.